Cameo2 Is Coordinated with CBP in Carotenoid Transport

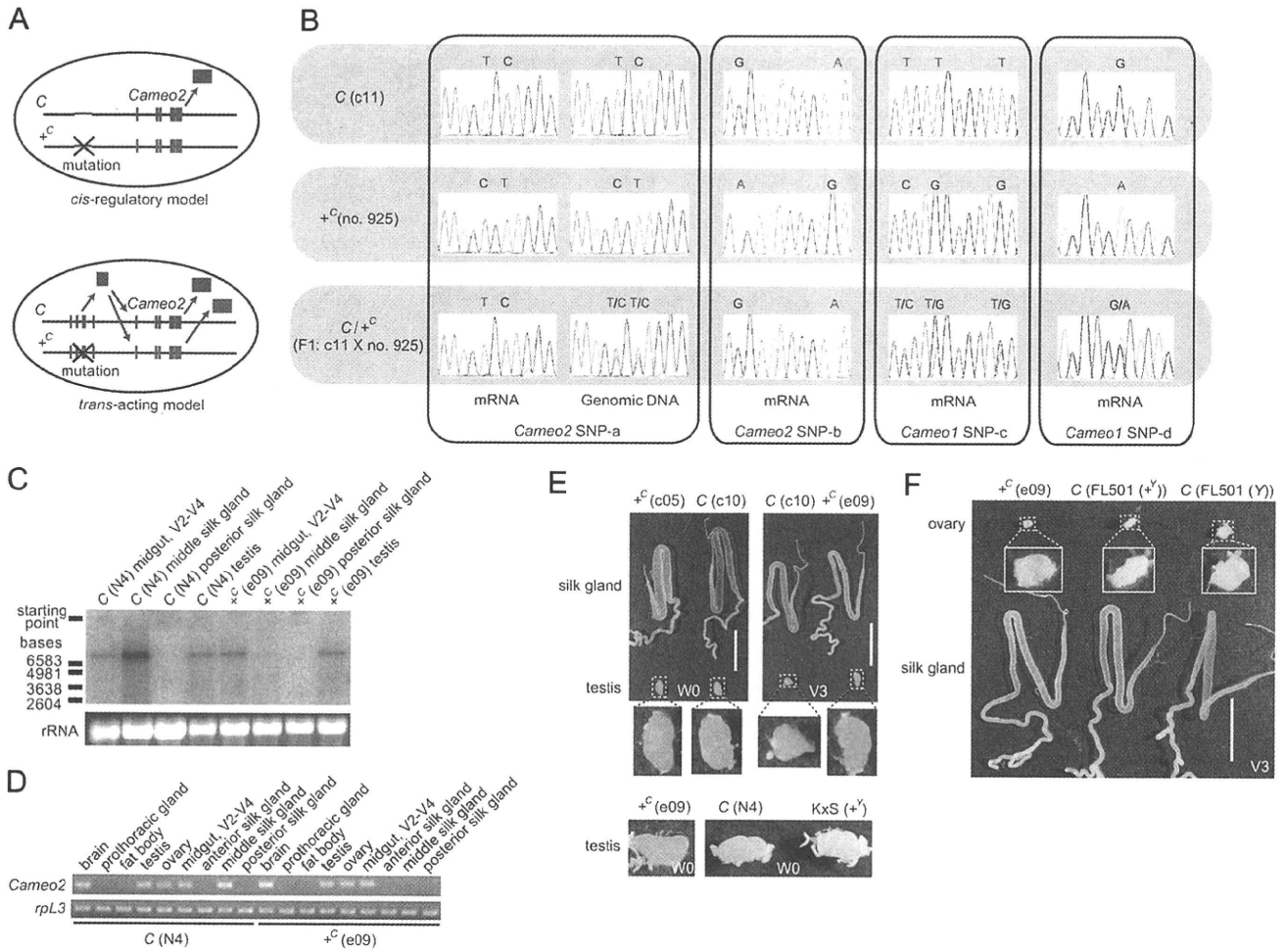

FIGURE 6. **The *C* locus controlled the *Cameo2* expression in a tissue-specific manner likely by a *cis*-regulatory manner.** *A*, schematic diagram of the principle of SNP analysis in F1 to elucidate whether *Cameo2* expression is controlled in a *cis*-regulatory or *trans*-acting manner. *B*, SNP analysis in *Cameo1* and *Cameo2* of the *C*, $+^C$, and F1 larvae. mRNA and genomic DNA were from the middle and posterior silk glands, respectively. The stage was V2–V4. The SNP sites are indicated in supplemental Fig. S2. Similar SNP patterns were obtained from three individuals of F1 larvae. *C* and *D*, examination of tissue distribution of *Cameo2* by Northern blotting (*C*) and RT-PCR (*D*) analyses. *rpL3* is an internal control (28). The stage was W0 unless otherwise noted. *E* and *F*, comparison of carotenoid pigmentation in the silk gland, testis, and ovary between the *C* and $+^C$ allele strains. Stages are indicated on the figures. *White* around the testis or ovary were fat body. *Scale bar*, 1 cm.

DISCUSSION

Recent improvements in the assembly of genome sequences (22) and physical marker resources (32, 33, 55) have made it feasible to clone mutant genes via positional cloning methods in the silkworm. Using these facilities, we attempted to elucidate the molecular identity of the *C* gene, a classical cocoon-color mutant gene mediating the cellular uptake of lutein in coordination with the *Y* gene in the middle silk gland (Fig. 1). Two paralogous membrane-spanning protein genes belonging to the CD36 gene family, *Cameo1* and *Cameo2*, were then cloned from the narrowed 375-kb interval of the *C*-linked region (see Figs. 2 and 3). Based on expression analysis (see Figs. 4 and 5) and transgenic rescue of the phenotype (see Fig. 7), the *C* gene is considered to encode Cameo2 and control the cellular uptake of lutein in the middle silk gland by regulating Cameo2 expression at a transcriptional level. The nucleotides responsible for the *C* mutation may correspond to a *cis*-regulatory element of *Cameo2*, which controls *Cameo2* expression in the middle silk gland in a specific manner (Fig. 6).

Based on the results presented here, along with those of previous studies of CBP, we propose a hypothetical transport pathway for lutein in the *C* and $+^C$ allele strains (see Fig. 7*F*). In the larval body of the *C* allele strain with the background of the *Y* allele, *Cameo2* is expressed in the midgut, middle silk gland, ovary, and testis. CBP is also expressed in these tissues (12, 13). Dietary mulberry leaves containing lutein are digested in the midgut lumen. Lutein is then absorbed into the midgut cells, possibly by Cameo2, and binds to CBP in the midgut cell to diffuse in the cytosol, which in turn transfers it to lipophorin in the hemolymph. Lipophorin reaches the middle silk gland and the genital organs via hemolymph, and then binds to the lipophorin receptor on each tissue. The lipophorin receptor on these tissues would be Cameo2 itself, another membrane receptor such as the vertebrate very low density lipoprotein receptor-like protein (56), or their complexes. Lutein is transported into these tissues by a membrane lutein transporter, which could be Cameo2 itself, where it binds to CBP in the cytosol again, resulting in yellow coloration of these tissues. In the $+^C$ allele strain

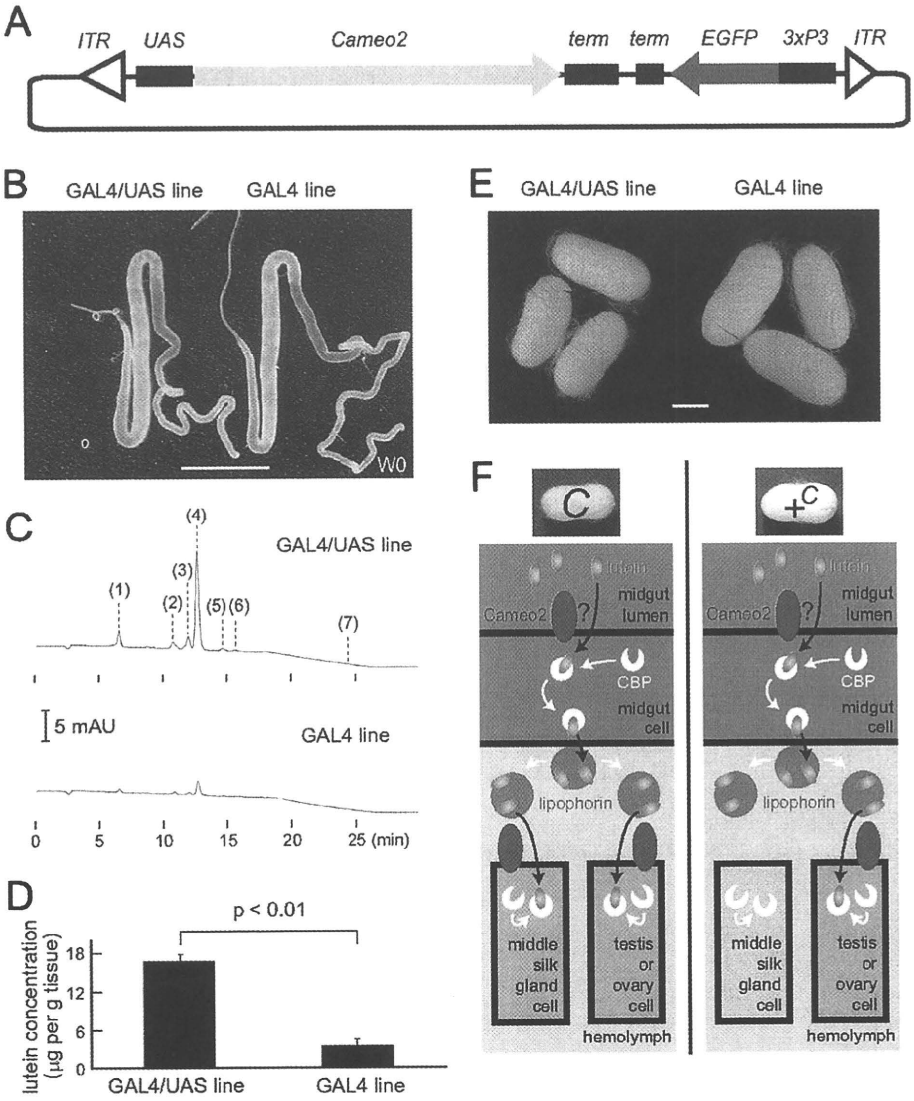

FIGURE 7. **Restoration of the phenotype of lutein accumulation by transgenic expression of *Cameo2*.** *A*, organization of the transgenic vector used. *ITR*, inverted terminal repeats of *piggyback*; *term*, SV40 terminator, *3xP3*, eye-specific promoter. *B*, silk glands of the GAL4/UAS (Ser1-GAL4/UAS-Cameo2) line, which was supposed to express Cameo2 in the middle silk gland by the binary system (30), and the GAL4 line as a control. The stage was W0. We confirmed similar stronger colorations in the GAL4/UAS line than the GAL4 line by observation of eight larvae of the GAL4/UAS line and 10 larvae of the GAL4 line. *C*, a representative chart of the reverse-phase HPLC analysis of carotenoid composition of the middle silk gland in the transgenic larvae. The stage was W0. Detection was at 474 nm. Peak positions 1, 2, 3, 4, 5, 6, and 7 correspond to the elution of 3′-dehydrolutein, 13-*cis*-lutein, unknown lutein derivative, lutein (trans lutein), zeaxanthin, 9-*cis*-lutein, and β-carotene, respectively. β-Carotene was barely detectable in the middle silk gland of the GAL4/UAS line. *D*, lutein concentration in the middle silk gland of the GAL4/UAS line and the GAL4 line (mean, S.E.; $n = 3$). The stage was W0. Statistical significance ($p < 0.01$) was analyzed by Student's *t* test. *E*, cocoon colors of the GAL4/UAS and GAL4 lines. All individuals analyzed in *B–E* exhibited the yellow hemolymph. *Scale bar*, 1 cm. *F*, model of the transport pathway for lutein in the larvae of the *C* and $+^C$ allele strains. Lutein is transported into the tissues where both Cameo2 and CBP express. Cameo2 in the internal organs would act as the lipophorin receptor and/or the membrane lutein transporter. See "Discussion" for details.

with the background of the *Y* allele, lutein would be similarly transferred to lipophorin and absorbed into the genital organs, whereas the middle silk gland rarely accumulates lutein due to its low level of Cameo2 expression. As both the CD36 family genes and the START domain-containing genes are prevalent in animals, coordination between them could also occur in other systems of selective lipid transport, as presumed for the mammalian steroidogenic system (36).

Although the midgut expresses both *Cameo2* and CBP, its feature in the cellular absorption of carotenoids is different from that of the middle silk gland as the midgut absorbs a certain amount of β-carotene in addition to lutein (8, 9). Although the present data do not deny the involvement of Cameo2 in the carotenoid absorption of the midgut, there would be other mechanisms/factors than those of the middle silk gland.

The function of Cameo1 remains elusive. Although the present results do not exclude the possibility that Cameo1 is involved in the cellular uptake of lutein, detection of *Cameo1* expression in broad tissues (see Figs. 5*D* and supplemental S4) implies that Cameo1 may be associated with a more ubiquitous function rather than tissue-specific control of lutein accumulation. It is noteworthy that tandem arrays of several paralogous genes of the CD36 gene family such as *Cameo1* and *Cameo2* are frequently observed in the silkworm (Fig. 3*D*) and Dipterans (48), whereas the physiological meaning of these tandem arrays is unknown.

Historically, the *C* mutant was originally found to produce white cocoons even though the color of hemolymph is yellow (57, 58). This was in contrast to the belief at that time that cocoon color is inevitably correlated with hemolymph color. The genetic mechanism of cocoon coloration by carotenoids has been investigated for biological and commercial purposes in part because cocoon-color genes are useful genetic markers for breeding that do not require sophisticated equipment, and cocoon colors impart distinctive color traits on some kinds of silk production. The present study identifies *Cameo2* as a molecular genetic tool for regulating cocoon color; however, the intensity of cocoon pigmentation by transgenic expression of *Cameo2* might not be enough to generate a convenient phenotype for breeding or commercial value (Fig. 7*E*). The weakness of coloration could, at least in part, be due to low uptake of lutein in the middle silk gland (Fig. 7*D*), which was 5–10-fold lower than that of the native *C* allele strain at W0 (data not shown). We expect that development of a more efficient

expression system for the transgene product in the middle silk gland would enhance the intensity of transgenic cocoon color.

Our results demonstrate that in one mutant of a membrane protein, the *Cameo2* mutant, lutein uptake of the middle silk gland is affected. One possible explanation for these observations is that Cameo2 is in the lutein-specific transfer factor present at the cell surface of the middle silk gland, which transports lutein from extracellular lipophorin to the intracellular CBP. A number of questions, however, remain. First, it is not yet known whether there are direct interactions between lipophorin and Cameo2 or Cameo2 and CBP. Although CLAMP (59), a PDZ domain-containing cytosolic protein, fatty acid-binding protein (60), and Src family proteins (61) have been suggested to have a physical interaction with the cytosolic region of SR-BI or CD36, they show no significant homology to CBP. Second, the site at which the selectivity for lutein is determined remains elusive. As the *Y* gene is involved in absorption of both lutein and β-carotene from the midgut lumen into midgut cells (8, 9) and combination of the *Y* gene and the *Flesh* gene, another cocoon-color mutant gene, facilitates the selective uptake of β-carotene in the posterior part of the middle silk gland (8, 62), the selectivity for lutein can be expected to be determined solely by Cameo2. However, the molecular properties of this CD36 family member that are responsible for lipid selectivity have yet to be determined. Biochemical and histological approaches with the *C* and *Y* mutants to these questions may reveal mechanisms by which dietary carotenoids are selectively transported to target tissues by relays of multiple factors to perform their diverse physiological functions.

Acknowledgments—We thank members of the Insect Genome Research Unit at National Institute of Agrobiological Sciences for technical assistance in the sampling of BF1 individuals for mapping and R. O. Ryan for critical reading of the manuscript.

REFERENCES

1. Goodwin, T. W. (1986) *Annu. Rev. Nutr.* **6,** 273–297
2. Loane, E., Nolan, J. M., O'Donovan, O., Bhosale, P., Bernstein, P. S., and Beatty, S. (2008) *Surv. Ophthalmol.* **53,** 68–81
3. Goldberg, I. J. (1996) *J. Lipid Res.* **37,** 693–707
4. Brown, M. S., and Goldstein, J. L. (1986) *Science* **232,** 34–47
5. Krieger, M. (1999) *Annu. Rev. Biochem.* **68,** 523–558
6. Oku, M. (1934) *Bull. Agric. Chem. Soc. Jap.* **10,** 1258–1262
7. Manunta, C. (1937) *Arch. Zool. Ital.* **24,** 385–401
8. Nakajima, M. (1963) *Bull. Fac. Agric. Tokyo Univ. Agric. Technol.* **8,** 1–80
9. Tsuchida, K., Katagiri, C., Tanaka, Y., Tabunoki, H., Sato, R., Maekawa, H., Takada, N., Banno, Y., Fujii, H., Wells, M. A., and Jouni, Z. E. (2004) *J. Insect Physiol.* **50,** 975–983
10. Van der Horst, D. J., and Ryan, R. O. (2004) in *Comprehensive Insect Physiology, Biochemistry, Pharmacology and Molecular Biology* (Gilbert, L. I., Iatrou, K., and Gill, S., eds) pp. 225–246, Elsevier, Oxford
11. Tazima, Y. (1964) *The Genetics of the Silkworm,* LOGOS Press, United Kingdom
12. Tabunoki, H., Sugiyama, H., Tanaka, Y., Fujii, H., Banno, Y., Jouni, Z. E., Kobayashi, M., Sato, R., Maekawa, H., and Tsuchida, K. (2002) *J. Biol. Chem.* **277,** 32133–32140
13. Tsuchida, K., Jouni, Z. E., Gardetto, J., Kobayashi, Y., Tabunoki, H., Azuma, M., Sugiyama, H., Takada, N., Maekawa, H., Banno, Y., Fujii, H., Iwano, H., and Wells, M. A. (2004) *J. Insect Physiol.* **50,** 363–372
14. Hara, W., Sosnicki, S., Banno, Y., Fujimoto, H., Takada, N., Maekawa, H., Fujii, H., Wells, M. A., and Tsuchida, K. (2007) *J. Insect Biotechnol. Seric.* **76,** 149–154
15. Sakudoh, T., Tsuchida, K., and Kataoka, H. (2005) *Biochem. Biophys. Res. Commun.* **336,** 1125–1135
16. Sakudoh, T., Sezutsu, H., Nakashima, T., Kobayashi, I., Fujimoto, H., Uchino, K., Banno, Y., Iwano, H., Maekawa, H., Tamura, T., Kataoka, H., and Tsuchida, K. (2007) *Proc. Natl. Acad. Sci. U.S.A.* **104,** 8941–8946
17. Alpy, F., and Tomasetto, C. (2005) *J. Cell Sci.* **118,** 2791–2801
18. Tsuchida, K., Arai, M., Tanaka, Y., Ishihara, R., Ryan, R. O., and Maekawa, H. (1998) *Insect Biochem. Mol. Biol.* **28,** 927–934
19. Harizuka, M. (1948) *J. Seric. Sci. Jap.* **17,** 1–5
20. Fujimoto, N. (1949) *J. Seric. Sci. Jap.* **18,** 82–87
21. Sturtevant, A. H. (1915) *Am. Nat.* **49,** 42–44
22. The International Silkworm Genome Consortium (2008) *Insect Biochem. Mol. Biol.* **38,** 1036–1045
23. Mita, K., Morimyo, M., Okano, K., Koike, Y., Nohata, J., Kawasaki, H., Kadono-Okuda, K., Yamamoto, K., Suzuki, M. G., Shimada, T., Goldsmith, M. R., and Maeda, S. (2003) *Proc. Natl. Acad. Sci. U.S.A.* **100,** 14121–14126
24. Rogers, M. E., Krieger, J., and Vogt, R. G. (2001) *J. Neurobiol.* **49,** 47–61
25. Tanaka, H., Ishibashi, J., Fujita, K., Nakajima, Y., Sagisaka, A., Tomimoto, K., Suzuki, N., Yoshiyama, M., Kaneko, Y., Iwasaki, T., Sunagawa, T., Yamaji, K., Asaoka, A., Mita, K., and Yamakawa, M. (2008) *Insect Biochem. Mol. Biol.* **38,** 1087–1110
26. Vogt, R. G., Miller, N. E., Litvack, R., Fandino, R. A., Sparks, J., Staples, J., Friedman, R., and Dickens, J. C. (2009) *Insect Biochem. Mol. Biol.* **39,** 448–456
27. Larkin, M. A., Blackshields, G., Brown, N. P., Chenna, R., McGettigan, P. A., McWilliam, H., Valentin, F., Wallace, I. M., Wilm, A., Lopez, R., Thompson, J. D., Gibson, T. J., and Higgins, D. G. (2007) *Bioinformatics* **23,** 2947–2948
28. Niwa, R., Sakudoh, T., Namiki, T., Saida, K., Fujimoto, Y., and Kataoka, H. (2005) *Insect Mol. Biol.* **14,** 563–571
29. Tamura, T., Thibert, C., Royer, C., Kanda, T., Abraham, E., Kamba, M., Komoto, N., Thomas, J. L., Mauchamp, B., Chavancy, G., Shirk, P., Fraser, M., Prudhomme, J. C., and Couble, P. (2000) *Nat. Biotechnol.* **18,** 81–84
30. Imamura, M., Nakai, J., Inoue, S., Quan, G. X., Kanda, T., and Tamura, T. (2003) *Genetics* **165,** 1329–1340
31. Tatematsu, K. I., Kobayashi, I., Uchino, K., Sezutsu, H., Iizuka, T., Yonemura, N., and Tamura, T. (September 30, 2009) *Transgenic Res.* 10.1007/s11248-009-9328-2
32. Yamamoto, K., Narukawa, J., Kadono-Okuda, K., Nohata, J., Sasanuma, M., Suetsugu, Y., Banno, Y., Fujii, H., Goldsmith, M. R., and Mita, K. (2006) *Genetics* **173,** 151–161
33. Yamamoto, K., Nohata, J., Kadono-Okuda, K., Narukawa, J., Sasanuma, M., Sasanuma, S. I., Minami, H., Shimomura, M., Suetsugu, Y., Banno, Y., Osoegawa, K., de Jong, P. J., Goldsmith, M. R., and Mita, K. (2008) *Genome Biol.* **9,** R21
34. Azhar, S., and Reaven, E. (2002) *Mol. Cell. Endocrinol.* **195,** 1–26
35. Martinez, L. O., Perret, B., Barbaras, R., Tercé, F., and Collet, X. (2007) in *High Density Lipoproteins* (Fielding, C. J., ed) pp. 307–338, Wiley-VCH Verlag GmbH & Co. KGaA, Weinheim
36. Connelly, M. A. (2009) *Mol. Cell. Endocrinol.* **300,** 83–88
37. Rodrigueza, W. V., Thuahnai, S. T., Temel, R. E., Lund-Katz, S., Phillips, M. C., and Williams, D. L. (1999) *J. Biol. Chem.* **274,** 20344–20350
38. Kiefer, C., Sumser, E., Wernet, M. F., and Von Lintig, J. (2002) *Proc. Natl. Acad. Sci. U.S.A.* **99,** 10581–10586
39. Voolstra, O., Kiefer, C., Hoehne, M., Welsch, R., Vogt, K., and von Lintig, J. (2006) *Biochemistry* **45,** 13429–13437
40. Wang, T., Jiao, Y., and Montell, C. (2007) *J. Cell Biol.* **177,** 305–316
41. van Bennekum, A., Werder, M., Thuahnai, S. T., Han, C. H., Duong, P., Williams, D. L., Wettstein, P., Schulthess, G., Phillips, M. C., and Hauser, H. (2005) *Biochemistry* **44,** 4517–4525
42. Reboul, E., Abou, L., Mikail, C., Ghiringhelli, O., André, M., Portugal, H., Jourdheuil-Rahmani, D., Amiot, M. J., Lairon, D., and Borel, P. (2005) *Biochem. J.* **387,** 455–461
43. During, A., Doraiswamy, S., and Harrison, E. H. (2008) *J. Lipid Res.* **49,** 1715–1724

44. Moussa, M., Landrier, J. F., Reboul, E., Ghiringhelli, O., Coméra, C., Collet, X., Fröhlich, K., Böhm, V., and Borel, P. (2008) *J. Nutr.* **138,** 1432–1436
45. Sonnhammer, E. L., von Heijne, G., and Krogh, A. (1998) *Proc. Int. Conf. Intell. Syst. Mol. Biol.* **6,** 175–182
46. Emanuelsson, O., Brunak, S., von Heijne, G., and Nielsen, H. (2007) *Nat. Protoc.* **2,** 953–971
47. Gruarin, P., Thorne, R. F., Dorahy, D. J., Burns, G. F., Sitia, R., and Alessio, M. (2000) *Biochem. Biophys. Res. Commun.* **275,** 446–454
48. Nichols, Z., and Vogt, R. G. (2008) *Insect Biochem. Mol. Biol.* **38,** 398–415
49. Franc, N. C., Heitzler, P., Ezekowitz, R. A., and White, K. (1999) *Science* **284,** 1991–1994
50. Philips, J. A., Rubin, E. J., and Perrimon, N. (2005) *Science* **309,** 1251–1253
51. Benton, R., Vannice, K. S., and Vosshall, L. B. (2007) *Nature* **450,** 289–293
52. Jin, X., Ha, T. S., and Smith, D. P. (2008) *Proc. Natl. Acad. Sci. U.S.A.* **105,** 10996–11001
53. Su, X., and Abumrad, N. A. (2009) *Trends Endocrinol. Metab.* **20,** 72–77
54. Fujimoto, N. (1943) *J. Seric. Sci. Jap.* **14,** 276–282
55. Miao, X. X., Xub, S. J., Li, M. H., Li, M. W., Huang, J. H., Dai, F. Y., Marino, S. W., Mills, D. R., Zeng, P., Mita, K., Jia, S. H., Zhang, Y., Liu, W. B., Xiang, H., Guo, Q. H., Xu, A. Y., Kong, X. Y., Lin, H. X., Shi, Y. Z., Lu, G., Zhang, X., Huang, W., Yasukochi, Y., Sugasaki, T., Shimada, T., Nagaraju, J., Xiang, Z. H., Wang, S. Y., Goldsmith, M. R., Lu, C., Zhao, G. P., and Huang, Y. P. (2005) *Proc. Natl. Acad. Sci. U.S.A.* **102,** 16303–16308
56. Gopalapillai, R., Kadono-Okuda, K., Tsuchida, K., Yamamoto, K., Nohata, J., Ajimura, M., and Mita, K. (2006) *J. Lipid Res.* **47,** 1005–1013
57. Ishii, K. (1917) *Sakurakai Zasshi.* **1,** 113–115
58. Uda, H. (1919) *Genetics* **4,** 395–416
59. Ikemoto, M., Arai, H., Feng, D., Tanaka, K., Aoki, J., Dohmae, N., Takio, K., Adachi, H., Tsujimoto, M., and Inoue, K. (2000) *Proc. Natl. Acad. Sci. U.S.A.* **97,** 6538–6543
60. Spitsberg, V. L., Matitashvili, E., and Gorewit, R. C. (1995) *Eur. J. Biochem.* **230,** 872–878
61. Huang, M. M., Bolen, J. B., Barnwell, J. W., Shattil, S. J., and Brugge, J. S. (1991) *Proc. Natl. Acad. Sci. U.S.A.* **88,** 7844–7848
62. Harizuka, M. (1953) *Bull. Seric. Exp. Sta. Jap.* **14,** 141–156
63. Zhao, Y. P., Li, M. W., Xu, A. Y., Hou, C. X., Li, M. H., Guo, Q. H., Huang, Y. P., and Guo, X. J. (2008) *Insect Sci.* **15,** 399–404
64. Hoosdally, S. J., Andress, E. J., Wooding, C., Martin, C. A., and Linton, K. J. (2009) *J. Biol. Chem.* **284,** 16277–16288

International Journal of Food Microbiology 143 (2010) 161–165

Contents lists available at ScienceDirect

International Journal of Food Microbiology

journal homepage: www.elsevier.com/locate/ijfoodmicro

Molecular identification of *Anisakis* type I larvae isolated from hairtail fish off the coasts of Taiwan and Japan

Azusa Umehara [a,b], Yasushi Kawakami [a], Hong-Kean Ooi [c,d], Akihiko Uchida [a], Hiroshi Ohmae [b], Hiromu Sugiyama [b,*]

[a] *Laboratory of Parasitology, School of Life and Environmental Science, Azabu University, 1-17-71 Fuchinobe, Chuo Ward, Sagamihara City, Kanagawa 229-8501, Japan*
[b] *Department of Parasitology, National Institute of Infectious Diseases, 1-23-1 Toyama, Shinjuku Ward, Tokyo 162-8640, Japan*
[c] *Department of Veterinary Medicine, National Chung Hsing University, 250 Kuo Kuang Road, Taichung 402, Taiwan*
[d] *Faculty of Agriculture, Yamaguchi University, 1677-1 Yoshida, Yamaguchi City, Yamaguchi 753-8515, Japan*

ARTICLE INFO

Article history:
Received 4 June 2010
Received in revised form 11 August 2010
Accepted 11 August 2010

Keywords:
Anisakis typica
Anisakis simplex sensu stricto
Anisakis pegreffii
Ribosomal DNA internal transcribed spacer
Hairtail

ABSTRACT

Anisakid nematodes are known to cause the zoonotic disease, anisakiasis, through the consumption of raw or undercooked fish. The parasites most frequently associated with the disease in humans are categorized as *Anisakis* type I, which comprise several species of the genus *Anisakis*. The larvae show primitive forms and lack the detailed morphological characteristics required for precise species identification. Thus, molecular characterization is necessary for determining the species of *Anisakis* type I larvae and acquiring important clinical and epidemiological information. In this study, we isolated *Anisakis* type I larvae from hairtail fish caught off the coasts of Taiwan and Japan. The ribosomal DNA (rDNA) internal transcribed spacer (ITS) region was sequenced, and restriction fragment length polymorphism (RFLP) analyses using *Hin*fI and *Hha*I was carried out for species identification. Most larvae isolated from hairtail caught in Taiwan were *Anisakis typica* (84%), while those isolated from hairtail caught in Japan were almost exclusively identified either as *Anisakis simplex* sensu stricto (65%) or *Anisakis pegreffii* (33%). This is the first report of *A. typica* in fish obtained from Taiwan. Our results shed the light on the epidemiology of *Anisakis* type I larvae, which is a potential cause of human anisakiasis in Taiwan and Japan.

1. Introduction

Larvae of anisakid nematodes are commonly found in marine fish and squid. Many cases of human anisakiasis caused by larvae belonging to the family Anisakidae have been reported in Japan and other countries due to the increasing popularity of eating raw fish (Lymbery and Cheah, 2007). Berland (1961) classified the larvae of anisakid nematodes into only two types, namely *Anisakis* types I and II, based on morphological characteristics such as the length of the ventriculus and presence/absence of mucron at the tip of the tail. The type I larvae were recognized as the parasite most frequently associated with human anisakiasis (Oshima, 1972; Smith and Wootten, 1978). Controversy regarding the species names of *Anisakis* type I and II larvae still remains because the larvae lack the detailed morphological characteristics required for precise species identification. The use of allozyme markers made it possible for the type I morphotypes to be identified as *Anisakis pegreffii*, *Anisakis simplex* sensu stricto, *Anisakis simplex* C, *Anisakis typica*, and *Anisakis ziphidarum* (Mattiucci et al., 1997, 2002; Paggi et al., 1998). The former three species have been recognized as sibling species belonging to *Anisakis simplex* sensu lato. The species comprising *Anisakis* types I and type II have also been characterized by sequencing and restriction fragment length polymorphism (RFLP) analyses of the ribosomal DNA (rDNA) internal transcribed spacer region (ITS region), namely the 5.8S rDNA and flanking ITS regions, ITS1 and ITS2 (Mattiucci and Nascetti, 2006, 2008). The classifications based on allozyme markers were fully consistent with the results obtained by these molecular methods.

It is imperative to identify *Anisakis* type I larvae detected in food fish in order to improve food safety. Hairtail is one of the most common and economically important food fish in the East and South China Seas. In Japan, Taiwan, and Korea, hairtail is often sold in markets and is favored for raw consumption as sashimi or sushi. However, few studies have investigated the molecular identification of anisakid larvae isolated from hairtail (Shih, 2004). Therefore, in this study, we detected *Anisakis* type I larvae in hairtail collected from Taiwan and Japan and applied these molecular methods for species identification.

2. Materials and methods

2.1. Parasite materials

Seven hairtail (*Trichiurus* spp.) specimens caught off the coast of each of the following 5 localities were examined for anisakid larvae:

* Corresponding author. Tel.: +81 3 5285 1111; fax: +81 3 5285 1173.
E-mail address: hsugi@nih.go.jp (H. Sugiyama).

0168-1605/$ – see front matter © 2010 Elsevier B.V. All rights reserved.
doi:10.1016/j.ijfoodmicro.2010.08.011

Taichung, Taiwan, and Nagasaki, Kochi, Wakayama and Shizuoka prefectures, Japan. We purchased the fish at retail fish markets in the respective localities, except for fish from Nagasaki, which were purchased from a retail fish market in Tokyo. Fish were examined immediately after transfer to our laboratory in Taichung (samples from Taiwan) or in Tokyo (samples from Japan).

Anisakid larvae were isolated from the visceral surface and body cavity of the fish. The larvae were observed under light and dissection microscopes for morphological identification (Ishii et al., 1989), and third-stage larvae of *Anisakis* type I were used for further molecular investigation.

2.2. DNA amplification

DNA samples were extracted from individual worms using a DNeasy Blood and Tissue Kit (Qiagen K. K., Tokyo, Japan) according to the manufacturer's instructions. The entire ITS region (ITS1, 5.8S rDNA and ITS2) was amplified by PCR using primers NC5 (forward; 5′-GTAGGTGAACCTGCGGAAGGATCATT-3′) and NC2 (reverse; 5′-TTAGTTTCTTTTCCTCCGCT-3′) (Abe et al., 2005). PCR was conducted using a mixed solution (5 μl) of extracted DNA as a template, with a reaction mixture (45 μl) containing 1.25 units of *TaKaRa EX Taq*, 1× PCR buffer (10 mM Tris-HCl pH 8.3, 50 mM KCl, 1.5 mM $MgCl_2$), 0.2 mM of each dNTP (Takara Bio Inc., Shiga, Japan) and 0.5 μM of each primer. PCR was performed using a LittleGene PCR machine (Bioer, Hangzhou, China) with 35 cycles as follows: denaturation at 98 °C for 5 s, annealing at 52 °C for 30 s, and extension at 72 °C for 60 s. A final extension was carried out at 72 °C for 10 min. The PCR products were separated by electrophoresis on 1.0% Seakem GTG agarose gels (Lonza Rockland, Inc., Rockland, ME, USA) in Tris-borate-EDTA buffer and visualized by illumination with short-wave ultraviolet light after ethidium bromide staining.

2.3. RFLP analysis

Restriction enzymes *Hin*fI and *Hha*I (New England Biolabs, Ipswithch, MA, USA) were used in the RFLP analysis for identifying the species of *Anisakis* type I, according to the genetic key of D'Amelio et al. (2000). The PCR products were digested according to the manufacturer's recommendations. The digested samples were then separated by electrophoresis on 2.0% Seakem GTG agarose gels (Lonza Rockland, Inc.) and visualized as previously described.

2.4. Sequencing

The PCR products were excised from the agarose gels and sequenced using a BigDye Terminator Cycle Sequencing Kit (Applied Biosystems Inc., Foster City, CA, USA) on an automated sequencer (ABI3100, Applied Biosystems). Sequence similarities were determined by a BLAST search of the DNA Data Bank of Japan (DDBJ) (http://blast.ddbj.nig.ac.jp/top-j.html). Sequence alignment and comparison was facilitated by the GENETYX-WIN program (ver.7.0, Software Development Co, Tokyo, Japan).

3. Results

3.1. Detection of Anisakis type I larvae from Taiwan and Japan

Six of the 7 hairtails from Taiwan and 15 of the 28 hairtails from Japan were positive for anisakid nematodes (Table 1), and 110 and 61 larvae were identified as *Anisakis* type I from these locations, respectively. The identification was based on the presence of a long ventriculus with an oblique ventricular-intestinal junction and a rounded tail possessing a mucron.

Table 1
Molecular identification of the *Anisakis* type I larvae.

Locality	Date of collection	No. of fish	No. of parasites			
		Infected/examined	Collected	Identified as		
				At[a]	Ap[b]	As[c]
Taiwan (Taichung)	14 Oct 2008	6/7	110	93	15	2
Japan (Nagasaki)	3 Dec 2008	5/7	20	0	20	0
Japan (Kochi)	13 Jul 2010	1/7	2	0	0	2
Japan (Wakayama)	18 Jul 2010	2/7	6	0	0	6
Japan (Shizuoka)	12 Jul 2010	7/7	33	1	0	32

[a] *A. typica*.
[b] *A. pegreffii*.
[c] *A. simplex* sensu stricto.

3.2. PCR-RFLP analysis

Amplification of the entire ITS region produced a single band of about 950 bp for all specimens. In RFLP, digestion of the PCR products with *Hin*fI produced three different RFLP patterns, corresponding to *A. typica* (ca. 590 and 330 bp), *A. pegreffii* (ca. 330, 280 and 240 bp), or *A. simplex* s. str. and *A. simplex* C (ca. 620 and 240 bp) (Fig. 1). For specimens showing the *A. simplex* s. str. and *A. simplex* C patterns, we then digested their respective PCR products only with *Hha*I and confirmed bands of ca. 530 and 420 bp for the *A. simplex* s. str. pattern (data not shown). Based on RFLP analyses of the 110 larvae from Taiwan, 93 (84%) were identified as *A. typica*, 15 (14%) were *A. pegreffii*, and 2 (2%) were *A. simplex* s. str. However, among 61 specimens from Japan, 40 (65%) were identified as *A. simplex* s. str., 20 (33%) were *A. pegreffii*, and 1 (2%) was *A. typica* (Table 1, Fig. 2).

3.3. Sequence of the entire ITS region

Entire ITS region sequences were determined for 5 larvae of *A. typica*, 5 larvae of *A. pegreffii*, and 1 larva of *A. simplex* s. str. from Taiwan as well as 1 larva of *A. typica* from Japan. No intraspecific differences were found in the sequences of these specimens. Similarity searches of the GenBank/EMBL/DDBJ nucleotide database revealed that the sequence of *A. typica* was identical to deposited sequences of the same species obtained at the larval stage from chub mackerel (*Scomber japonicus*, accession number AB432908) and at the

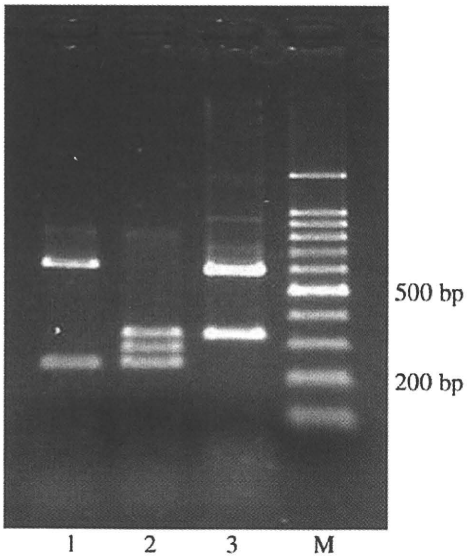

Fig. 1. RFLP analysis with *Hin*fI of the ITS PCR products amplified from the *Anisakis* type I larvae. Lane 1: *A. simplex* sensu stricto; Lane 2: *A. pegreffii*; Lane 3: *A. typica*. The 100-bp DNA ladder marker was used to estimate the size of the bands (lane M).

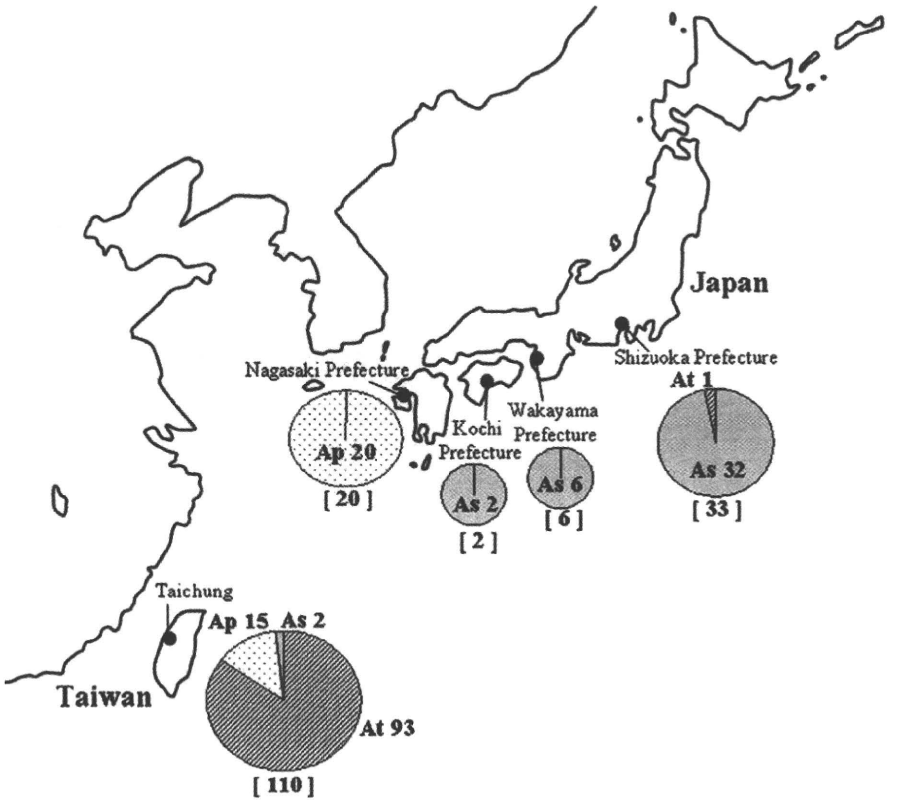

Fig. 2. Distribution of *A. typica* (At), *A. pegreffii* (Ap) and *A. simplex* sensu stricto (As) isolated from hairtail caught in coastal areas of Taiwan and Japan. Pie charts show the distribution of *Anisakis* type I larvae based on analysis of the rDNA ITS region. The numbers in square brackets and after the abbreviations of the species (At, Ap and As) represent the number of larvae examined and identified, respectively.

adult stage from rough-toothed dolphin (*Steno bredanensis*, AB479120). The nucleotide sequence of *A. typica* from Taiwan determined in this study has been deposited in the DDBJ/EMBL/GenBank database under the accession number AB551660. The sequences of *A. pegreffii* and *A. simplex* s. str. were also found to be identical to deposited sequences of each species obtained from chub mackerel (*S. japonicus*, AB277823) and arabesque greenling (*Pleurogrammus azonus*, AB277822), respectively.

The ITS sequence of *A. simplex* reported by Shih (2004) was not available from the GenBank/EMBL/DDBJ (shown in Fig. 3). Shih also isolated larvae for sequencing analysis from hairtail from Taiwan. Comparison with the sequence obtained in this study revealed that the sequence reported by Shih was 99% and 77% similar to those of *A. typica* and *A. simplex* s. str., respectively (Fig. 3).

4. Discussion

Anisakiasis is a zoonotic disease caused by the ingestion of anisakid nematodes in raw or undercooked fish. In previous reports, almost all the larvae recovered from humans have been identified as *Anisakis* type I based on their morphological characteristics (Oshima, 1972; Smith and Wootten, 1978). Since *Anisakis* type I is a morphotype comprising several species of the genus *Anisakis*, molecular characterization of *Anisakis* type I larvae is necessary for identifying each clinically and epidemiologically important species.

In this study, we observed that most of the larvae isolated from hairtail specimens from Taiwan were that of *A. typica*. To the best of our knowledge, this is the first report of *A. typica* in fish from Taiwan. In addition, a larva of *A. typica* was first detected in a hairtail specimen from Japan, though this species has been isolated from mackerel in Japan (Umehara et al., 2008a; Suzuki et al., 2010). In Asian countries besides Taiwan and Japan, *A. typica* has been reported in China, Korea, Indonesia and Thailand (Zhu et al., 2007; Chen et al., 2008; Palm et al., 2008; Lee et al., 2009; Du et al., 2010).

Shih (2004) reported the isolation of anisakid larvae from hairtail from Taiwan and sequenced the rDNA ITS region. Surprisingly, the so-called *A. simplex* sequence determined by Shih had a 99% similarity to the sequence of *A. typica* in this study. This implies that the sequence of anisakid larvae reported by Shih was probably that of *A. typica*, and not of *A. simplex*. According to the review by Mattiucci and Nascetti (2006, 2008), *A. typica* is widely distributed between 30°S and 35°N in warm and tropical waters. Nevertheless, there have been few reports of *A. typica* detected in both paratenic host fish and definitive host marine mammals. Kagei (2003) reported that the number of worms of *A. typica* in the definitive host was less than that for *A. simplex*. The lack of reports of *A. typica* might also be due to insufficient recognition of the species and hence misidentification of *A. typica* as *A. simplex*.

The sequence of *A. typica* obtained in this study was identical to the two sequences already deposited in the GenBank/EMBL/DDBJ (AB432908 and AB479120). However, when compared with the sequence reported by Shih as *A. simplex*, the *A. typica* sequence differed by 4 nucleotides in the ITS1 region and 1 nucleotide in the ITS2 region. Previous studies have reported geographical intraspecific variations in the entire ITS region of *A. typica* from Indonesia and Brazil (Palm et al., 2008, Iñiguez et al., 2009). This may indicate that some genotypes of *A. typica* are globally distributed in the ocean.

Japanese people traditionally eat fish raw as sushi and sashimi, and over 2000 cases of human anisakiasis are estimated to occur annually (Chai et al., 2005). In Taiwan, consumption of raw fish is also a common practice, and anisakiasis is therefore an important consideration. However, only one case has been reported in Taiwan to date, and the causative pathogen was not identified (Ishikura, 2003).

Fig. 3. Alignment of the entire ITS region sequences of *A. typica*. As (Shih, 2004), the sequence incorrectly reported as *A. simplex*; At (AB432908), the sequence obtained from larva isolated from chub mackerel; At (AB479120), the sequence obtained from adults isolated from rough-toothed dolphin; At (present study), the sequence obtained from larva isolated from hairtail in Taiwan in this study (AB551660). Asterisk (*) indicates identity to the reference sequence. GenBank/EMBL/DDBJ accession numbers are each shown in parentheses, where applicable.

We recently identified the species of the *Anisakis* type I larvae isolated from fish and from anisakiasis patients in Japan (Umehara et al., 2006, 2007, 2008b). Although both *A. simplex* s. str. and *A. pegreffii* were detected in fish, almost all larvae (99%) from patients were identified as *A. simplex* s. str. In other words, there is a striking discrepancy in the predominant species between fish and humans. Suzuki et al. (2010) explained that this was due to the higher penetration rate of *A. simplex* s. str. into the muscle tissue of the fish. *A. simplex* s. str. larvae were therefore ingested by humans together with the fish muscles, while *A. pegreffii* larvae were usually removed from the fish along with the internal organs prior to ingestion.

To date, although *A. typica* has not been recorded as a cause of human anisakiasis and the risk of human infection by *A. typica* has been assumed to be low, Palm et al. (2008) reported the isolation of a single larva of *A. typica* from the musculature of the bullet tuna (*Auxis rochei rochei*). Since *A. typica* is the predominant species in the hairtail

found in the coastal waters of Taiwan, there is always a possibility of human cases outbreak in that country where people have recently begun to eat raw hairtail. As it is not possible to distinguish *A. typica* from the other *Anisakis* type I larvae through morphology, molecular methods are indispensable for determining the incidence of *A. typica* infection in humans. This is important not only in Taiwan, but also in other countries where the presence of *A. typica* and other species comprising the *Anisakis* type I has been noted.

Acknowledgements

We thank Dr. Stefano D'Amelio of the University of Rome 'La Sapienza' and Dr. Nelio Barros of the Mote Marine Laboratory for supplying adult specimens of *Anisakis typica*. Dr. Hiroshi Yamasaki, Dr. Yasuyuki Morishima and Dr. Masanori Kawanaka of the National Institute of Infectious Diseases, Dr. Jun Araki of the Meguro Parasitological Museum and Dr. Kazuo Nakamura of Kitasato University provided invaluable suggestions and encouragement throughout this study. This research was supported in part by grants for Research on Emerging and Re-emerging Infectious Diseases from the Ministry of Health, Labor and Welfare of Japan. This research was also partially supported by the Promotion and Mutual Aid Corporation for Private Schools of Japan, Grant-in-Aid for Matching Fund Subsidy for Private Universities.

References

Abe, N., Ohya, N., Yanagiguchi, R., 2005. Molecular characterization of *Anisakis pegreffii* larvae in pacific cod in Japan. Journal of Helminthology 79, 303–306.

Berland, B., 1961. Nematodes from some Norwegian marine fishes. Sarsia 2, 1–50.

Chai, J.Y., Murrell, K.D., Lymbery, A.J., 2005. Fish-borne parasitic zoonoses: status and issues. International Journal for Parasitology 35, 1233–1254.

Chen, Q., Yu, H.Q., Lun, Z.R., Chen, X.G., Song, H.Q., Lin, R.Q., Zhu, X.Q., 2008. Specific PCR assays for the identification of common anisakid nematodes with zoonotic potential. Parasitology Research 104, 79–84.

D'Amelio, S., Mathiopoulos, K.D., Santos, C.P., Pugachev, O.N., Webb, S.C., Picanco, M., Paggi, L., 2000. Genetic markers in ribosomal DNA for the identification of members of the genus *Anisakis* (Nematoda: Ascaridoidea) defined by polymerase chain reaction-based restriction fragment length polymorphism. International Journal for Parasitology 30, 223–226.

Du, C., Zhang, L., Shi, M., Ming, Z., Hu, M., Gasser, R.B., 2010. Elucidating the identity of *Anisakis* larvae from a broad range of marine fishes from the Yellow Sea, China, using a combined electrophoretic-sequencing approach. Electrophoresis 31, 654–658.

Iñiguez, A.M., Santos, C.P., Vicente, A.C., 2009. Genetic characterization of *Anisakis typica* and *Anisakis physeteris* from marine mammals and fish from the Atlantic Ocean off Brazil. Veterinary Parasitology 165, 350–356.

Ishii, Y., Fujino, T., Weerasooriya, M.V., Ishii, Y., Fujino, T., Weerasooriya, M.V., 1989. Morphology of anisakine larvae. In: Ishikura, H., Namiki, M., Ishikura, H., Namiki, M. (Eds.), Gastric Anisakiasis in Japan. Epidemiology, Diagnosis, Treatment. Springer-Verlag, Tokyo, pp. 19–29.

Ishikura, H., 2003. Anisakiasis (2) clinical pathology and epidemiology. In: Otsuru, M., Kamegai, S., Hayashi, S. (Eds.), Progress of Medical Parasitology in Japan. Meguro Parasitological Museum, Tokyo, pp. 451–473.

Kagei, N., 2003. Anisakiasis. (1) Biology. In: Otsuru, M., Kamegai, S., Hayashi, S. (Eds.), Progress of Medical Parasitology in Japan. Meguro Parasitological Museum, Tokyo, pp. 421–449.

Lee, M.H., Cheon, D.S., Choi, C., 2009. Molecular genotyping of *Anisakis* species from Korean sea fish by polymerase chain reaction-restriction fragment length polymorphism (PCR-RFLP). Food Control 20, 623–626.

Lymbery, A.J., Cheah, F.Y., 2007. Anisakid nematodes and anisakiasis. In: Murrell, K.D., Fried, B. (Eds.), Food-borne Parasitic Zoonoses. Springer, US, pp. 185–207.

Mattiucci, S., Nascetti, G., 2006. Molecular systematics, phylogeny and ecology of anisakid nematodes of the genus *Anisakis* Dujardin, 1845: an update. Parasite 13, 99–113.

Mattiucci, S., Nascetti, G., 2008. Advances and trends in the molecular systematics of anisakid nematodes, with implications for their evolutionary ecology and host-parasite co-evolutionary processes. Advances in Parasitology 66, 47–148.

Mattiucci, S., Nascetti, G., Clanchi, R., Paggi, L., Arduino, P., Margolis, L., Brattey, J., Webb, S., D'Amelio, S., Orecchia, P., Bullini, L., 1997. Genetic and ecological data on the *Anisakis simplex* complex, with evidence for a new species (Nematoda, Ascaridoidea, Anisakidae). The Journal of parasitology 83, 401–416.

Mattiucci, S., Paggi, L., Nascetti, G., Portes Santos, C., Costa, G., Di Beneditto, A.P., Ramos, R., Argyrou, M., Cianchi, R., Bullini, L., 2002. Genetic markers in the study of *Anisakis typica* (Diesing, 1860): larval identification and genetic relationships with other species of *Anisakis* Dujardin, 1845 (Nematoda: Anisakidae). Systematic parasitology 51, 159–170.

Oshima, T., 1972. *Anisakis* and anisakiasis in Japan and adjacent areas. In: Morishita, K., Komiya, Y., Matsubayashi, H. (Eds.), Progress of Medical Parasitology in Japan. Meguro Parasitological Museum, Tokyo, pp. 305–393.

Paggi, L., Nascetti, G., Webb, S.C., Mattiucci, S., Cianchi, R., Bullini, L., 1998. A new species of *Anisakis* Dujardin, 1845 (Nematoda, Anisakidae) from beaked whales (Ziphiidae): allozyme and morphological evidence. Systematic Parasitology 40, 161–174.

Palm, H.W., Damriyasa, I.M., Linda, Oka, I.B.M., 2008. Molecular genotyping of *Anisakis* Dujardin, 1845 (Nematoda: Ascaridoidea: Anisakidae) larvae from marine fish of Balinese and Javanese waters, Indonesia. Helminthologia 45, 3–12.

Shih, H.H., 2004. Parasitic helminth fauna of the cutlass fish, *Trichiurus lepturus* L., and the differentiation of four anisakid nematode third-stage larvae by nuclear ribosomal DNA sequences. Parasitology Research 93, 188–195.

Smith, J.W., Wootten, R., 1978. *Anisakis* and anisakiasis. Advances in Parasitology 16, 93–163.

Suzuki, J., Murata, R., Hosaka, M., Araki, J., 2010. Risk factors for human *Anisakis* infection and association between the geographic origins of *Scomber japonicus* and anisakid nematodes. International Journal of Food Microbiology 137, 88–93.

Umehara, A., Kawakami, Y., Araki, J., Uchida, A., 2006. Molecular identification of *Anisakis simplex* sensu stricto and *Anisakis pegreffii* (Nematoda: Anisakidae) from fish and cetacean in Japanese waters. Parasitology International 55, 267–271.

Umehara, A., Kawakami, Y., Araki, J., Uchida, A., 2007. Molecular identification of the etiological agent of the human anisakiasis in Japan. Parasitology International 56, 211–215.

Umehara, A., Sugiyama, H., Kawakami, Y., Uchida, A., Araki, J., 2008a. Identification of *Anisakis simplex* larvae from fish in Japanese market at the sibling species level. Clinical Parasitology 19, 114–117 (in Japanese).

Umehara, A., Kawakami, Y., Araki, J., Uchida, A., Sugiyama, H., 2008b. Molecular analysis of Japanese *Anisakis simplex* worms. The Southeast Asian Journal of Tropical Medicine and Public Health 39 (Suppl. 1), 26–31.

Zhu, X.Q., Podolska, M., Liu, J.S., Yu, H.Q., Chen, H.H., Lin, Z.X., Luo, C.B., Song, H.Q., Lin, R.Q., 2007. Identification of anisakid nematodes with zoonotic potential from Europe and China by single-strand conformation polymorphism analysis of nuclear ribosomal DNA. Parasitology Research 101, 1703–1707.

Parasitol Res (2010) 107:1003–1007
DOI 10.1007/s00436-010-1961-4

SHORT COMMUNICATION

A human case of subcutaneous dirofilariasis caused by *Dirofilaria repens* in Vietnam: histologic and molecular confirmation

Thi Cam Thach Dang · Thu Huong Nguyen · Trung Dung Do · Shoji Uga · Yasuyuki Morishima · Hiromu Sugiyama · Hiroshi Yamasaki

Received: 28 April 2010 / Accepted: 14 June 2010 / Published online: 1 July 2010

Abstract Human dirofilariasis caused by infection with *Dirofilaria* worms has been frequently reported. The symptoms associated with infection by these filarial parasites, which are transmitted to humans by zooanthropophilic mosquitoes, are characterized by mainly pulmonary and subcutaneous nodules. Here, we report the first case in Vietnam of a subcutaneous dirofilariasis with a painful nodule in the right eyelid. An immature female worm was removed by excisional biopsy and identified as *Dirofilaria repens* by histology and DNA analysis.

Nucleotide sequence data reported in the present paper are deposited in the DDBJ/GenBank/EMBL databases under the accession numbers AB547465 and AB547466 for the cytochrome c oxidase subunit 1 and 12S rRNA genes, respectively.

T. C. T. Dang (✉) · T. H. Nguyen · T. D. Do
Department of Parasitology, National Institute of Malariology, Parasitology and Entomology,
No. 245, Luong The Vinh street, Tu Liem,
BC 10200 Hanoi, Vietnam
e-mail: dtcthach@gmail.com

T. H. Nguyen
e-mail: ngocly1404@yahoo.com.vn

T. D. Do
e-mail: giudung77@gmail.com

S. Uga
Department of Parasitology,
Kobe University Graduate School of Health Sciences,
Kobe 654-0142, Japan
e-mail: ugas@kobe-u.ac.jp

Y. Morishima · H. Sugiyama · H. Yamasaki
Department of Parasitology,
National Institute of Infectious Diseases,
Tokyo 162-8640, Japan

Y. Morishima
e-mail: morisima@nih.go.jp

H. Sugiyama
e-mail: hsugi@nih.go.jp

H. Yamasaki
e-mail: hyamasak@nih.go.jp

Introduction

The genus *Dirofilaria* (Nematoda; Filarioidea, Onchocercidae), which includes etiologic agents such as *Dirofilaria immitis*, *Dirofilaria repens*, *Dirofilaria tenuis*, and *Dirofilaria ursi*, is responsible for the increased occurrence of zoonotic dirofilariasis in humans around the world (Pampiglione and Rivasi 2000). Of these species, *D. repens* is a habitual parasite in the subcutaneous tissue of dogs and other carnivores that are transmitted by zooanthropophilic mosquitoes (Culicidae). Human infections by this parasite also occur and more than 780 cases have been reported in over 37 countries in Europe, Southeast Asia, and Africa (Pampiglione et al. 1995; Pampiglione and Rivasi 2000). In Asia, human cases of *D. repens* infection have been reported in Iran, India, Sri Lanka, Malaysia, Thailand, China (Pampiglione and Rivasi 2000) and Japan (McLean et al. 1979), but such case has not yet been reported in Vietnam. In its definitive hosts, *D. repens* can easily be identified by its morphological features; however, in non-definitive hosts such as humans, these filarial worms may be more difficult to identify using morphological and histological characteristics, particularly when the clinical samples that have been removed from the subcutaneous nodules have become damaged and/or immature worms were found (Pampiglione et al. 1999). Serological examination is a useful tool for differentiating between *D. repens*

and *D. immitis* infections (Santamaría et al. 1995), while elevated levels of IgM, IgG and IgE have been used in patients exposed to other *Dirofilaria* species (Simón et al. 1997; Orihel and Eberhard 1998). In order to overcome the limitations associated with serological and histological examinations, polymerase chain reaction (PCR)-based methods capable of differentiating between *Dirofilaria* species have been developed (Favia et al. 1996, 1997a, b, 2000; Rivasi et al. 2006; Marušić et al. 2008). Here, we report the first human case of *D. repens* infection in Vietnam, diagnosed definitively by histology and PCR-based DNA analysis.

Case report

The patient was a 30-year-old Vietnamese man residing in the Ha Dong district of Hanoi, the capital of Vietnam. In 2008, the patient presented at Ha Dong Hospital complaining of a painful, itchy, swollen and tangible nodule, measuring 1.0×0.5 cm on the right eyelid. The patient was treated with an antibiotic for the first week, but the clinical symptoms did not change. No routine laboratory data, such as white blood and eosinophil counts in blood were available. On April 19, 2008, surgical biopsy was performed with the aim of diagnosis and treatment. As a result, a long, slender, whitish and living worm, approximately 4.5 cm in length and 0.5 mm in width, was removed (Fig.1a) and clinical signs disappeared after the biopsy. The removed worm was fixed in 10% formalin and was kept at the National Institute of Malariology, Parasitology and Entomology (NIMPE) in Hanoi, Vietnam before being sent to the Department of Parasitology, National Institute of Infectious Diseases in Tokyo, Japan for identification of the parasite to the species level in 2009.

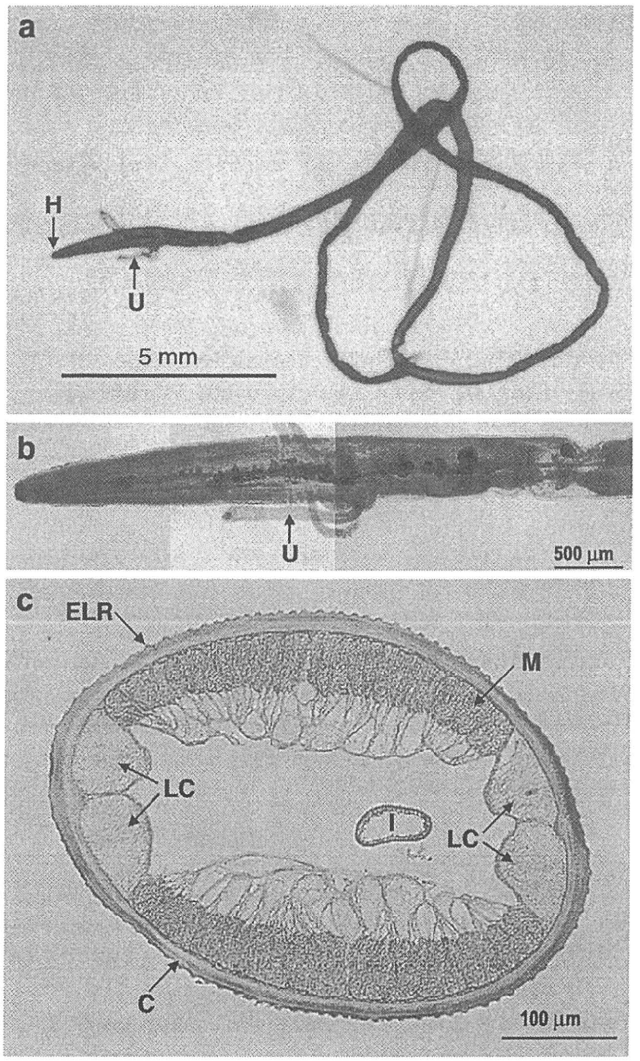

Fig. 1 Microscopic appearance and transverse section of the filarial worm surgically removed from the subcutaneous tissue of a human eyelid. **a** Removed immature female measuring approximately 4.5 cm in length and 500 μm in width. *H* head, *U* uterus. **b** Magnification of the anterior end of the worm. **c** Transverse section of the worm. Note the conspicuous external longitudinal ridges (*ELR*), polymyarian-type musculature (*M*), enlarged lateral chords (*LC*), multilayered cuticle (*C*), and intestine (*I*). Hematoxylin-eosin stain

Materials and methods

A part of the formalin-fixed worm kept at the NIMPE was processed for paraffin-embedded specimen and then transverse sections were stained with hematoxylin and eosin and were observed microscopically.

To confirm the morphological identification, molecular analysis was performed as follows: the remaining worm was homogenized in a small amount of the ATL buffer supplied with a DNeasy Blood & Tissue kit (Qiagen, Germany) before DNA was extracted overnight using the same kit. The mitochondrial cytochrome c oxidase subunit 1 (cox1) and 12S ribosomal RNA (12S rRNA) genes of the parasite were then amplified by PCR. Since the DNA samples were degraded by formalin fixation, short DNA sequences were amplified using the following primer pairs: Diro cox1/F255 (5′-GGTGCTATTAATTTTATGGTTACT-3′) and Diro cox1/R434 (5′-AAAAGAAGTATTAAAATTACGATC-3′), which were designed based on the cox1 gene sequences of *D. repens* (AM749234) and *D. immitis* (EU159111); and Diro 12S rRNA/F196 (5′-GTTTTGTTTAAACCGAA AAAATATT-3′) and Diro 12S rRNA/R374 (5′-TAAGCCA AATATATATCTGTTTTAA3′), which were designed based on the 12S rRNA gene sequences of *D. repens* (AJ544832) and *D. immitis* (EU182327). In addition, the following three primer pairs specific for 12S rRNA gene of *D. repens* were also used: Dr/F1 (5′-TCATTTTAATTTTTAACTC TATTT-3′) and Dr/R160 (5′-ATTAATAAACTTTGATTA

CCTGGG-3′), Dr/F121 (5′-TTGAACTGGATTAG TAACCCAGGT-3′) and Dr/R284 (5′-CTAAACAATCA TACATGTGCCAATA-3′), and Dr/F260 (5′-TATTGGCA CATGTATGATTGTTTAG-3′) and Dr/R443 (5′-CACAT AAGAAAAAATTCTTTCTT-3′), which were designed based on accession number AJ544832. PCR amplification of the target DNAs was performed in a 50-μL reaction mixture with Ex Taq DNA polymerase (Hot Start version, Takara Bio, Japan) and 35 cycles was performed consisting of denaturation (94°C, 30 s), annealing (58°C, 30 s) and extension (72°C, 60 s), with a final elongation step of 72°C for 5 min. The amplicons were confirmed by capillary electrophoresis (HAD-GT12, eGene Inc., CA) and were purified for use as templates for direct DNA sequencing using a NucleoSpin Extract II kit (Macherey-Nagel, Germany). Samples for sequencing were prepared using an ABI PRISM BigDye Terminator Cycle Sequencing Ready Reaction Kit (Applied Biosystems Inc., CA) and sequencing was performed on an ABI PRISM 3100-Avant Genetic Analyzer (Applied Biosystems Inc., CA). Sequence data were analyzed using the EditSeq and MegAlign programs of the DNASTAR package Inc. (DNASTAR, Madison, WI).

Results and discussion

The parasite exhibited movement at the time of surgical extraction. The body length measured 4.5 cm because the posterior part of the body was lacking (Fig. 1a). The uterus, which was protruding from the anterior end of the body at the time of removal, did not contain any larval microfilariae (Fig. 1a, b). A transverse section of the parasite (Fig. 1c) revealed that the parasite had a diameter of approximately 400 μm, a thick, laminated cuticle with external longitudinal ridges (99 ridges all around the nematode surface), and a well-developed, polymyarian-type musculature interrupted by two large lateral chords, all of which are characteristic of immature *D.* (*Nochtiella*) *repens* female worms.

In the molecular analysis, the target DNAs were successfully amplified by nested PCR using primer pairs specific for *D. repens*, but not primer pairs specific for *D. immitis* (data not shown). Figure 2 shows the alignment of the PCR-amplified cox1 (a, 123 bp) and 12S rRNA genes (b, 362 bp) nucleotide sequences. Homology search revealed sequence similarities of 97.6% and 91.1% against the cox1 genes of the *D. repens* (AM749233) and *D. immitis* reference sequences (EU159111), respectively. For the 12S rRNA gene, homology with the *D. repens* reference sequence (AM779772) reached as high as 99.2%; whereas, homology with the *D. immitis* reference sequence (EU182327) was lower at 85.9 %. In addition, the obtained sequence data also confirmed that the filarial worm in this case was *D. repens*.

Considerable variation has been observed in the dimensions of male and female *D. repens* recovered from a variety of definitive hosts around the world. Compared with other *Dirofilaria* worms, the *D. repens* is a robust parasite with a maximum female and male body length of 17 cm and approximately 7 cm, respectively and a diameter of 650 μm and 450 μm, respectively, have been reported

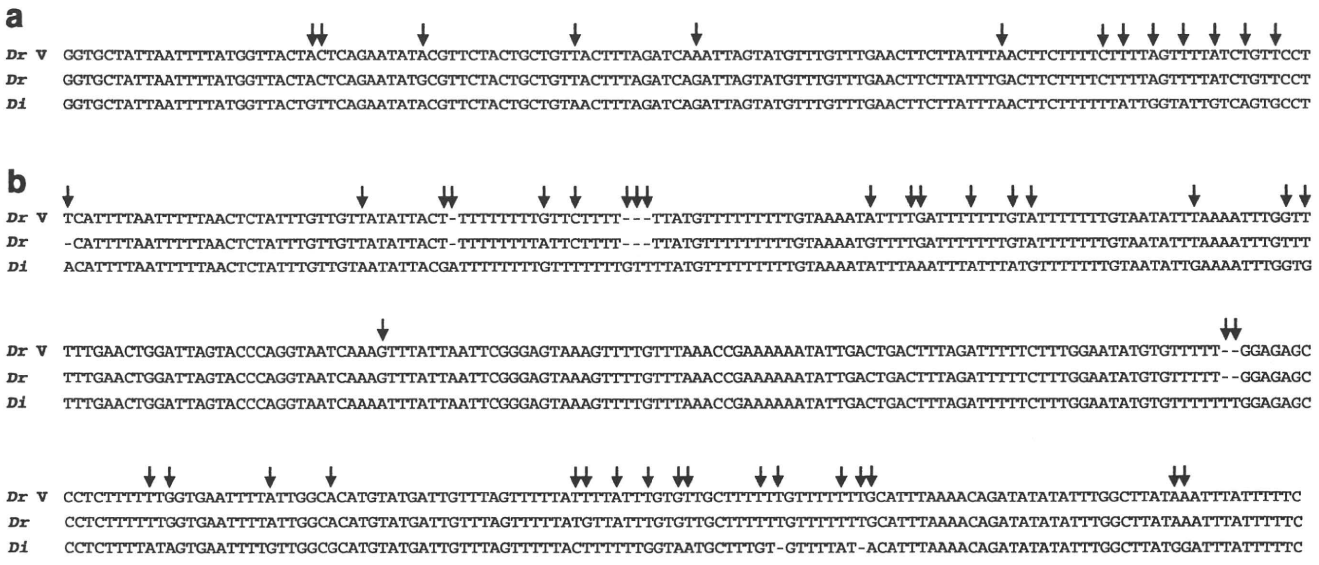

Fig. 2 Alignment of the PCR-amplified cox1 and 12S rRNA gene sequences. **a** Cox1 gene; *Dr V, D. repens* obtained from a Vietnamese patient; *Dr, D. repens* (AM749233); and *Di, D. immitis* (EU159111). **b** 12S rRNA gene; *Dr V, D. repens* from this case; *Dr, D. repens* (AM779772); *Di, D. immitis* (EU182327). *Arrows* indicate differences between nucleotides of *D. repens* and *D. immitis*

(Orihel and Eberhard 1998). In cases of human infection, *D. repens* measuring up to approximately 660 μm in diameter have been observed (Gutierrez 1984; Pampiglione et al. 1995). In this case, the maximum body width measured approximately 500 μm. Although an extensive review of human infections by *D. repens* found that female worms were more prevalent than males (Pampiglione and Rivasi 2000), a male and a female worm have been observed in the same nodule (Mrad et al. 1999), and also in separate nodules (Fernando et al. 2000). In the majority of cases, nodules are located in subcutaneous and subconjunctival tissues, deep dermis and submucosa. According to Pampiglione and Rivasi (2000), localization is more frequent in the upper half of the body (74%), mostly in the ocular region (35.3%) and the upper limbs (11%). Although rare, localization in muscle tissue, lymph nodes (Maltezos et al. 2002) and in the deep viscera (Pampiglione and Rivasi 2000) has been reported. In this case, the nodule was located in the eyelid.

The identification of *Dirofilaria* worms can only be made with certainty after a biopsy. The morphological features of individual parasites are as follows: body length and width, thickness of the laminated cuticle, the presence and/or absence of external longitudinal ridges on the surface of the cuticle, lateral chords, and number and type of circumferential muscle cells (Orihel and Eberhard 1998; Ratnatunga and Wijesundera 1999; Pampiglione et al. 1999). However, depending on the quality of the histological sections, some of these morphological features may not be absolute. In addition, identification of the causative *Dirofilaria* agent is also closely correlated with geographic areas affected with individual *Dirofilaria* species (Orihel and Eberhard 1998).

The most precise method for identifying *Dirofilaria* worms is, therefore, molecular identification using biopsied tissues and/or parasite material. Several PCR-based diagnostic methods have been developed using DNA samples prepared from fresh and ethanol-fixed tissues (Chandrasekharan et al. 1994; Favia et al. 1996, 1997a, 2000; Cancrini et al. 1998; Vakalis et al. 1999, 2002), as well as formalin-fixed and paraffin-embedded specimens (Favia et al. 1997a; Vakalis et al. 1999, 2002; Rivasi et al. 2006; Marušić et al. 2008). These PCR-based approaches target the internal transcribed spacer two region and tandemly repeated sequence of the cuticular surface antigen gene. The combination of the PCR-based assay with DNA sequencing of the mitochondrial DNA (cox1 and 12S rRNA genes) using formalin-fixed specimens reported here is considered to be useful for the precise identification of the *Dirofilaria* species. Such DNA analyses are useful not only for diagnostic investigations, but also for retrospective studies using histopathological specimens fixed in formalin (Yamasaki et al. 2007).

Acknowledgements This work was conducted as part of a core university program between Vietnam and Japan sponsored by the Japan Society for Promotion of Sciences. This work was also supported in part by a grant-in-aid from the Ministry of Health, Labour, and Welfare, Japan (H20-Shinko-Ippan-016).

References

Chandrasekharan NV, Karunanayake EH, Franzen L, Abeyewickreme W, Pettersson U (1994) *Dirofilaria repens*: cloning and characterization of repeated DNA sequence for the diagnosis of dirofilariasis in dogs, *Canis familiaris*. Exp Parasitol 78:279–286

Cancrini G, Favia G, Giannetto S, Merulla R, Russo R, Ubaldino V, Tringai R, Pietrobelli M, Del Nero L (1998) Nine more cases of human infection by *Dirofilaria repens* diagnosed in Italy by morphology and recombinant DNA technology. Parassitologia 40:461–466

Favia G, Lanfrancotti A, Della Torre A, Cancrini G, Coluzzi M (1996) Polymerase chain reaction—identification of *Dirofilaria repens* and *D. immitis*. Parasitology 113:567–571

Favia G, Lanfrancotti A, Della Torre A, Cancrini G, Coluzzi M (1997a) Advances in the identification of *Dirofilaria repens* and *Dirofilaria immitis* by a PCR-based approach. Parassitologia 39:401–402

Favia G, Tringali R, Cancrini G (1997b) Molecular diagnosis of human dirofilariasis. Ann Trop Med Parasitol 91:961–962

Favia G, Cancrini G, Ricci I, Bazzocchi C, Magi M, Pietrobelli M, Genchi C, Bandi C (2000) 5S ribosomal spacer sequences of some filarial parasites: comparative analysis and diagnostic applications. Mol Cell Probes 14:285–290

Fernando SD, Ihalamulla RL, De Silva WAS (2000) Male and female filarial worms *Dirofilaria* (*Nochtiella*) *repens* recovered from the scrotum. Ceylon Med J 45:131–132

Gutierrez Y (1984) Diagnostic features of zoonotic filariae in tissue sections. Hum Pathol 15:514–525

Maltezos ES, Sivridis EL, Giatromanolaki AN, Simopoulos CE (2002) Human subcutaneous dirofilariasis: a report of three cases manifesting as breast or axillary nodules. Scott Med J 47:86–88

Marušić Z, Stastny T, Kirac I, Stojčević D, Krušlin B, Tomas D (2008) Subcutaneous dirofilariasis caused by *Dirofilaria repens* diagnosed by histopathologic and polymerase chain reaction analysis. Acta Dermatovenerol Croat 16:222–225

McLean JD, Beaver PC, Michalek H (1979) Subcutaneous dirofilariasis in Okinawa, Japan. Am J Trop Med Hyg 28:45–48

Mrad K, Romani-Ramah S, Driss M, Bougrine F, Hechiche M, Maalej M, Romdhane KB (1999) Mammary dirofilariasis. A case report. Int J Surg Pathol 7:175–178

Orihel TC, Eberhard ML (1998) Zoonotic filariasis. Clin Micrbiol Rev 11:366–381

Pampiglione S, Rivasi F (2000) Human dirofilariasis due to *Dirofilaria* (*Nochtiella*) *repens*: an update of world literature from 1995 to 2000. Parassitologia 42:231–254

Pampiglione S, Canestri Trotti G, Rivasi F (1995) Human dirofilariasis due to *Dirofilaria* (*Nochtiella*) *repens*: a review of world literature. Parassitologia 37:149–193

Pampiglione S, Rivasi F, Canestri-Trotti G (1999) Pitfalls and difficulties in histological diagnosis of human dirofilariasis due to *Dirofilaria* (*Nochtiella*) *repens*. Diagn Microbiol Infect Dis 34:57–64

Ratnatunga NVI, de Wijesundera MS (1999) Histopathological diagnosis of subcutaneous *Dirofilaria repens* infection in humans. Southeast Asian J Trop Med Public Health 30:375–378

Rivasi F, Boldorini R, Criante P, Leutner M, Pampiglione S (2006) Detection of *Dirofilaria* (*Nochtiella*) *repens* DNA by polymerase chain reaction in embedded paraffin tissues from two human pulmonary locations. APMIS 114:567–574

Santamaría B, Di Sacco B, Muro A, Genchi C, Simón F, Cordero M (1995) Serological diagnosis of subcutaneous dirofilariasis. Clin Exp Dermatol 20:19–21

Simón F, Prieto G, Muro A, Cancrini G, Cordero M, Genchi C (1997) Human humoral response to *Dirofilaria* species. Parassitologia 39:397–400

Vakalis N, Spanakos G, Patsoula E, Vamvakopoulos NC (1999) Improved detection of *Dirofilaria repens* DNA by direct polymerase chain reaction. Parasitol Int 48:145–150

Vakalis N, Vougioukas N, Patsoula E, Spanakos G, Sioutopoulou DO, Vamvakopoulos NC (2002) Genotypic assignment of infection by *Dirofilaria repens*. Parasitol Int 51:163–169

Yamasaki H, Nakaya K, Nakao M, Sako Y, Ito A (2007) Significance of molecular diagnosis using histopathological specimens in cestode zoonoses. Trop Med Health 35:307–321

International Journal for Parasitology 40 (2010) 1651–1658

Contents lists available at ScienceDirect

International Journal for Parasitology

journal homepage: www.elsevier.com/locate/ijpara

Paragonimus westermani possesses aerobic and anaerobic mitochondria in different tissues, adapting to fluctuating oxygen tension in microaerobic habitats

Shinzaburo Takamiya [a,*], Koich Fukuda [b], Takeshi Nakamura [c], Takashi Aoki [a], Hiromu Sugiyama [d]

[a] Department of Molecular and Cellular Parasitology, Graduate School of Medicine, Juntendo University, 2-1-1 Hongo, Bunkyo-ku, Tokyo 113-8421, Japan
[b] Center for Laboratory Animal Science, National Defense Medical College, 359 Tokorozawa, Japan
[c] Department of Parasitology, Kitasato University School of Medicine, Kanagawa 252-0374, Japan
[d] Department of Parasitology, National Institute of Infectious Diseases, Toyama 1-23-1, Shinjuku-ku, Tokyo 162-8640, Japan

ARTICLE INFO

Article history:
Received 26 April 2010
Received in revised form 1 July 2010
Accepted 2 July 2010

Keywords:
Aerobic and anaerobic mitochondria
Respiratory chain
Paragonimus westermani
NADH-fumarate reductase system
Tegument
Parenchyma

ABSTRACT

We previously showed that adult *Paragonimus westermani*, the causative agent of paragonimiasis and whose habitat is the host lung, possesses both aerobic and anaerobic respiratory chains, i.e., cyanide-sensitive succinate oxidase and NADH-fumarate reductase systems, in isolated mitochondria (Takamiya et al., 1994). This finding raises the intriguing question as to whether adult *Paragonimus* worms possess two different populations of mitochondria, one having an aerobic succinate oxidase system and the other an anaerobic fumarate reductase system, or whether the worms possess a single population of mitochondria possessing both respiratory chains (i.e., mixed-functional mitochondria). Staining of trematode tissues for cytochrome *c* oxidase activity showed three types of mitochondrial populations: small, strongly stained mitochondria with many cristae, localised in the tegument and tegumental cells; and two larger parenchymal cell mitochondria, one with developed cristae and the other with few cristae. The tegumental and parenchymal mitochondria could be separated by isopycnic density-gradient centrifugation and showed different morphological characteristics and respiratory activities, with low-density tegumental mitochondria having cytochrome *c* oxidase activity and high-density parenchymal mitochondria having fumarate reductase activity. These results indicate that *Paragonimus* worms possess three different populations of mitochondria, which are distributed throughout trematode tissues and function facultatively, rather than having mixed-functional mitochondria.

1. Introduction

Parasitic helminths including nematodes, trematodes and cestodes exhibit a variety of metabolic pathways (Tielens and van den Bergh, 1993; Komuniecki and Komuniecki, 1995; Behm, 2002; Kita and Takamiya, 2002). Their life cycle consists of two stages, a free-living larval stage that lives in an aerobic environment and a parasitic stage inside a host, in which oxygen tension depends on the tissues penetrated by migrating larvae or dwelt in by adult parasites. For example, the adult stage of *Ascaris suum*, a nematode that parasitises swine, dwells in the lumen of host small intestine, where oxygen tension is very low, while its fertilised eggs develop aerobically to form infective L3s. Therefore, during development parasitic helminths undergo aerobic–anaerobic transitions in energy metabolism resulting from adaptation to their environments. During its aerobic larval stage, *A. suum* possesses a functional tricarboxylic acid (TCA) cycle and a cyanide-sensitive respiratory chain similar to those in mammals (Takamiya et al., 1993; Amino et al., 2003; Iwata et al., 2008); both of these are localised in mitochondria and produce ATP by oxidative phosphorylation. That is, electrons derived from substrate oxidation are transported via NADH or flavin adenine dinucleotide (FADH) to oxygen by the proton-pumping electron-transfer complexes of the respiratory chain, and a proton gradient formed across the inner membrane drives ATP-synthase, resulting in ATP production with a backflow of protons. The respiratory chain consists of four electron-transfer complexes, i.e., complexes I (NADH-ubiquinone oxidoreductase), II (succinate-ubiquinone oxidoreductase, SQR), III (ubiquinol-cytochrome *c* oxidoreductase), and IV (cytochrome *c* oxidase, CCO), and two low-molecular weight electron carriers, cytochrome *c* and ubiquinone. Complexes I, III and IV have proton-pumping activity. Thus, mitochondria that produce ATP at the expense of oxygen can be defined as aerobic mitochondria, with 38 mol of ATP produced during the complete oxidation of each mol of glucose. Adult *Ascaris* nematodes, however, possess anaerobic mitochondria that yield ATP in the absence of oxygen.

* Corresponding author. Tel.: +81 3 5802 1043; fax: +81 3 5800 0476.
E-mail address: stakamiy@juntendo.ac.jp (S. Takamiya).

0020-7519/$36.00 © 2010 Australian Society for Parasitology Inc. Published by Elsevier Ltd. All rights reserved.
doi:10.1016/j.ijpara.2010.07.009

Mitochondria from adult *Ascaris* muscle have reduced levels of complex III and cytochrome *c*, and almost completely lack complex IV. These nematode mitochondria catalyze the NADH-dependent reduction of fumarate, which is endogenously derived from malate dismutation and serves as a terminal electron acceptor. NADH-linked fumarate reduction is mediated by complex I and by complex II, an isoform of the larval complex II (Takamiya et al., 1986). The latter, together with rhodoquinone, catalyzes rhodoquinol-fumarate reduction, the reverse of the succinate oxidation mediated by the larval enzyme, a reaction coupled to site 1 phosphorylation of ADP. Using this pathway, approximately 5 mol of ATP are produced per mol of glucose; a value higher than that for lactate fermentation (2 mol ATP per mol glucose) but lower than that observed using the aerobic pathway. Since adult *Ascaris* mitochondria can produce ATP by oxidative phosphorylation in the absence of oxygen, they are termed "anaerobic" mitochondria or more precisely, "anaerobically functioning mitochondria". Similar anaerobic mitochondria are present not only in parasitic helminths but also in other hypoxically functioning eukaryotes that live in microaerobic environments such as marine or freshwater sediments (Van Hellemond et al., 1995; Tielens et al., 2002). Therefore, oxygen tension where anaerobic mitochondria function is quite varied from extremely anoxic to less hypoxic or microaerobic. Although the molecular properties of anaerobic mitochondria, especially of their respiratory chains, have been elucidated in detail, the mechanisms of aerobic–anaerobic transition still remain to be determined with respect to mitochondrial biogenesis.

Paragonimus spp., lung flukes that infect mammals including humans, may provide appropriate material to investigate aerobic–anaerobic transitions in mitochondria. Adult *Paragonimus westermani* and *Paragonimus ohirai* inhabit mammalian lungs by forming cysts, in which oxygen tension fluctuates much more than in the lumen of the small intestine. We previously showed that the mitochondria of adult flukes possess both aerobic and anaerobic respiratory chains, i.e., mammalian-type, cyanide-sensitive respiratory chains and the NADH-fumarate reductase system (Ma et al., 1987; Takamiya et al., 1994). This finding raises the interesting question as to whether the adult *Paragonimus* spp. possess separate populations of aerobic and anaerobic mitochondria or a single mitochondrial population containing both the succinate oxidase and NADH-fumarate reductase systems. Our cytochemical study using *P. ohirai* supported the former view but we did not have sufficient biochemical evidence (Fujino et al., 1996). We have therefore attempted to separate the aerobic and anaerobic mitochondria, and to further characterise each individually.

2. Materials and methods

2.1. Isolation of P. westermani mitochondria

Adult *P. westermani* (3*n* type, 62 or 88 worms) were obtained from worm cysts from the lungs of dogs 8 or 12 months after inoculation with metacercariae. After removal of ovary tissue, the mitochondria were prepared as described (Takamiya et al., 1994). All procedures performed on laboratory animals were approved by the institutional animal care and use committee of the National Defense Medical College, Japan (the approval No. 09097) and all the animal experiments were carried out in compliance with the guidelines for animal experimentation of National Defense Medical College.

2.2. Isopycnic density-gradient centrifugation

Continuous 26 ml-sucrose density gradients, 32–52% (w/w) or 35–55% (w/w) containing 10 mM Tris–HCl, pH 7.5, 1 mM EDTA and 0.1% BSA were prepared using a density gradient fractionator (DGF-U, Hitachi, Japan). A mitochondrial suspension (0.9–1.2 ml) was loaded onto each gradient, which was centrifuged at 108,000*g* for 2 h in a Hitachi RP70T rotor at 4 °C. The contents of each tube were fractionated through the fractionator and CCO (Takamiya et al., 1994), fumarate reductase (FRD) (Kita et al., 1988) and SQR (Takamiya et al., 1994) activities, and the protein contents of these fractions, were measured. Using one drop of each fraction, the buoyant density was measured by measuring the sucrose concentration of each fraction with Abbe's refractometer and comparing each with a curve relating sucrose concentration to density. For protein assays, a 0.1 ml aliquot of each fraction was suspended in 0.9 ml of 0.025 M Tris–HCl buffer, pH 7.5, containing 0.21 M mannitol, 0.07 M sucrose and 0.1 mM EDTA. The suspensions were centrifuged at 14,000*g* for 15 min (Tomy MRX 150) to remove BSA and recover the mitochondria in the pellet. The supernatant was thoroughly removed and the protein content of each pellet was assayed (Markwell et al., 1978). For quinone determination, mitochondrial fractions were diluted with 10 vol. of 10 mM Tris–HCl, pH 7.4, containing 0.2 mM EDTA and the mixtures were centrifuged at 100,000*g* for 1 h to recover the mitochondrial particles. Each pellet was suspended in a small volume of the same buffer and used for quinone determination (Takamiya et al., 1994).

2.3. Electron microscopy

For cytochemical studies of CCO, worm tissues were fixed for 20 min at 4 °C in phosphate-buffered 2% glutaraldehyde, which had been purified overnight using active carbon. Small blocks of tissue were rinsed for several hours in the same buffer with 7% sucrose and sectioned at 40 μm on a Sorvall TC-2 tissue sectioner. The sections were collected in the same buffer and incubated for 2 h in medium (Seligman et al., 1968) at 37 °C. Control sections were incubated with the inhibitor, 10 mM KCN. The tissues were post-fixed for 45 min at 4 °C in 1% osmium tetroxide buffered to pH 7.4 with 0.05 M Veronal buffer and washed for 30 min with 0.1 M sodium acetate. Before dehydration with ethanol, the tissues were stained for 30 min in 0.5% uranyl acetate at 4 °C and examined using a JEOL JEM 100c electron microscope. Electron micrographs at magnifications of 5,000–10,000 were prepared to measure the maximum cross-sectional length and width and areas of mitochondria in trematode cells. The size of mitochondria in the micrographs were recorded using analysis Five software (Soft Imaging System GmbH, Münster, Germany).

Isolated mitochondria were fixed in 4% glutaraldehyde buffered with 10 mM Tris–HCl (pH 7.4), 0.21 M mannitol, 0.07 M sucrose and 0.1 mM EDTA, post-fixed in 1% osmium tetroxide in the same solution, dehydrated in ethanol, embedded in Quetal 812, and cut into sections of thickness 300–500 Å. These sections were stained with 4% uranyl acetate, treated with lead citrate hydroxide and examined under a Hitachi H-7,000 transmission electron microscope.

Electron micrographs at magnification 7,000 were prepared to measure the areas (μm^2) and brightness of cross-sections of individual fractionated mitochondria. The micrographs were examined using a computer-controlled image analyzer (KS400, Zeiss, Germany) equipped with a scanner (Epson GT-9100). Typically, for each fraction, 476–502 mitochondrial cross-sections were analyzed.

2.4. Statistical analyses

The areas and brightness of mitochondrial cross-sections were analyzed by Kaleida Graph ver. 4. For in situ observation, statistical analyses were performed using Prism 4 software (GraphPad Software, Inc., San Diego, CA, USA). Differences between means were

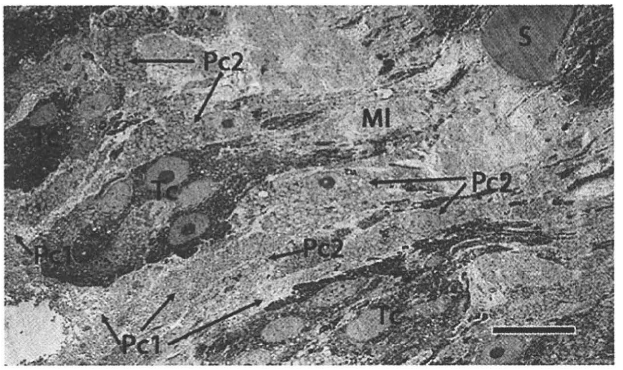

Fig. 1. Low magnification electron micrograph of the *Paragonimus* body wall. Ml, muscle layer; Pc1, parenchymal type-1 cells; Pc2, parenchymal type-2 cells; S, spine; T, tegument; Tc, tegumental cells. The magnification is 1000×. Scale bar = 20 μm.

analyzed using the Mann–Whitney *U*-test. $P < 0.05$ was considered statistically significant.

3. Results

3.1. In situ morphological features

Examination of the body wall sections of *P. westermani* by transmission electron microscopy showed that body wall cells could be categorised into two types, tegumental and parenchymal cells, based on their shape, the density of their cytoplasm and the number and morphology of mitochondria (Fig. 1). The morphological features of the two cell types were similar to those described for *P. ohirai*; the parenchymal cells could be further divided into two types, parenchymal cells types-1 and -2 (Pc1 and Pc2, respectively) (Fujino et al., 1996). Pc1, with cytoplasm less dense than that of Pc2, contain a few round or oval mitochondria with several long cristae in rather dense matrices (Fig. 2A). In contrast, Pc2 possess

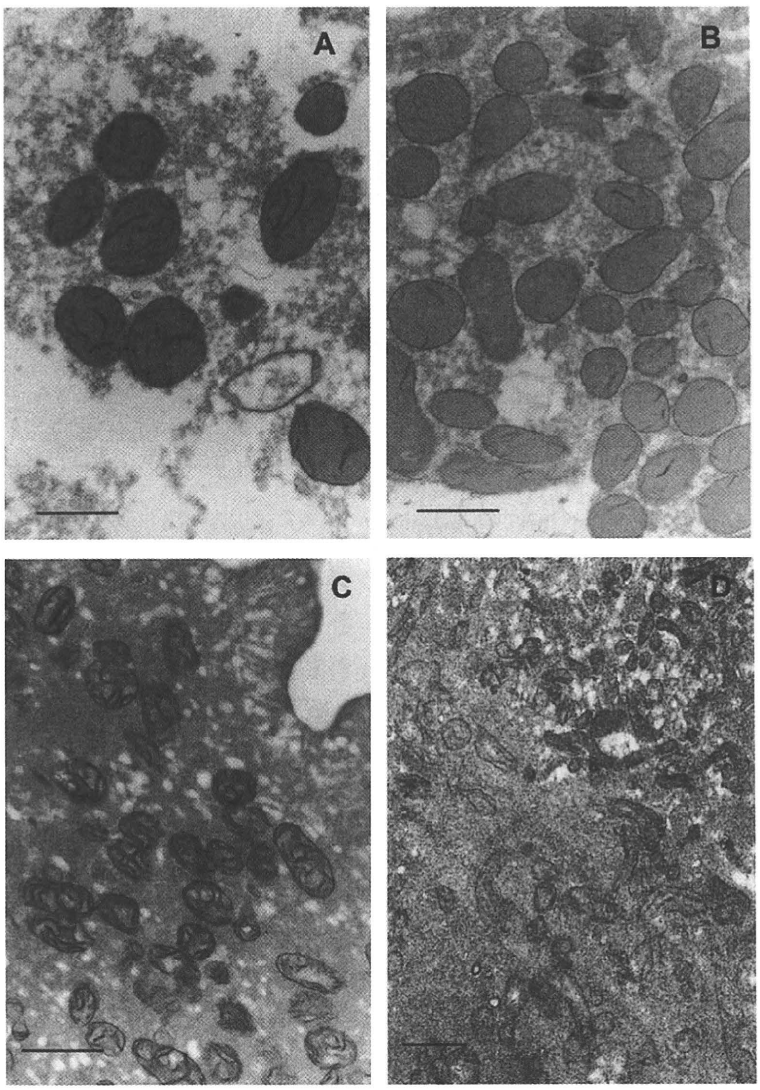

Fig. 2. Cytochrome *c* oxidase (CCO) staining of *Paragonimus* mitochondria in the (A) parenchymal type-1 cells; (B) parenchymal type-2 cells; and (C) tegument. (D) Tegumental cells for control. No significant staining was observed in the presence of KCN, a potent inhibitor of CCO. The magnification for A–C and D is 10,000× and 2,000×, respectively. Inserted bar represents 1 μm.

Table 1
In situ morphology of *Paragonimus westermani* mitochondria.

Sourc	Cross-section area (μm²)	Shape	Crista development	Matrix density	CCO staining
T or Tc	0.130 ± 0.0819	Oval	Well	Dense	Heavy
Pc1	0.330 ± 0.193	Round or oval	Moderate	Dense	Moderate
Pc2	0.350 ± 0.197	Round or oval	Poor	Less dense	Little

Cross-section areas (n = 190) were measured as described in Section 2.
T, tegument; Tc, tegumental cells; Pc1, parenchymal type-1cells; Pc2, parenchymal type-2 cells; CCO, cytochrome *c* oxidase.

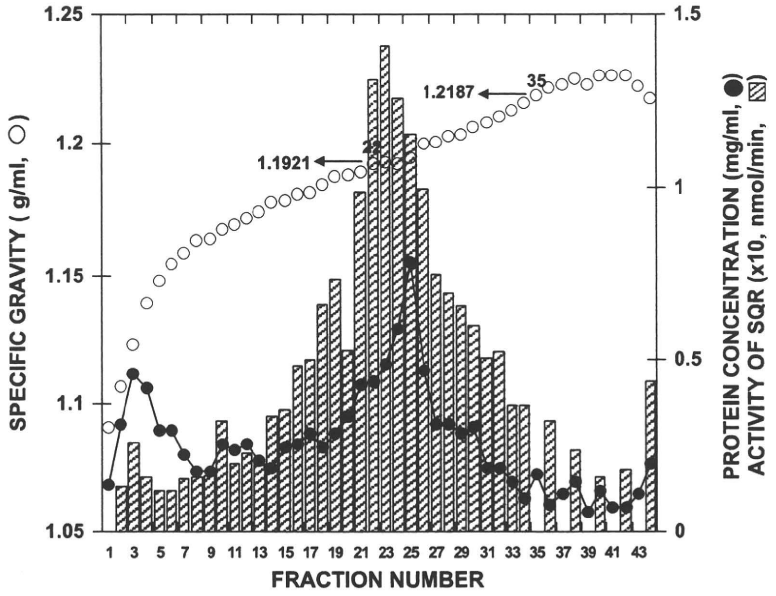

Fig. 3. Distribution of isolated *Paragonimus* mitochondria on isopycnic density gradient (32–52% (w/w) sucrose) centrifugation. Trematode mitochondria (10.0 mg protein) were centrifuged and the specific gravity (open circles), protein concentrations (closed circles), and activity of succinate-ubiquinone oxidoreductase (SQR) (shaded bars) were determined in each fraction. Mitochondria with high fumarate reductase (FRD)/cytochrome *c* oxidase ratios were present in Fractions 22–35. Detailed experimental procedures are described in Section 2.

numerous mitochondria, round or oval in shape, with less dense matrices than Pc1 and poorly developed cristae (Fig. 2B). Since the cristae of Pc1 mitochondria were positive for CCO, the terminal oxidase that reduces molecular oxygen, Pc1 mitochondria appear more aerobic than Pc2 mitochondria. In contrast to the parenchymal cells, the tegumental cells contain many small mitochondria with well-developed cristae and heavily positive for CCO activity (Fig. 2C). Therefore, among the three types of body wall mitochondria, the tegumental mitochondria appear most aerobic. Morphological features of *P. westermani* body wall mitochondria are summarised in Table 1.

3.2. Buoyant density and SQR activity of mitochondria fractionated by isopycnic density-gradient centrifugation

Paragonimus westermani mitochondria were analyzed by sucrose density-gradient centrifugation between 32% (w/w) and 50% (w/w) sucrose, with two gradient ranges, a low-density gradient range (1.0914–1.1546 g/ml) of Fractions 1–6 and a high density gradient range (1.1546–1.2267 g/ml) of Fractions 6–42. Since the density of 32% (w/w) sucrose solution is 1.1426 g/ml, higher than those for Fractions 1–4 (1.0914–1.1390 g/ml), the steep initial gradient was formed by dilution with sucrose–mannitol medium used to suspend mitochondria. The mitochondria were layered on top of the gradient.

Using SQR activity as the mitochondrial marker enzyme, *P. westermani* mitochondria were distributed at sucrose densities of 1.123–1.2267 g/ml (Fractions 2–42) with a main protein peak at 1.1946 g/ml (Fraction 25) (Fig. 3). The low-density peak at Fractions 2–4 contained small mitochondria with well-developed cristae, although cross-contaminating microsomal vesicles were

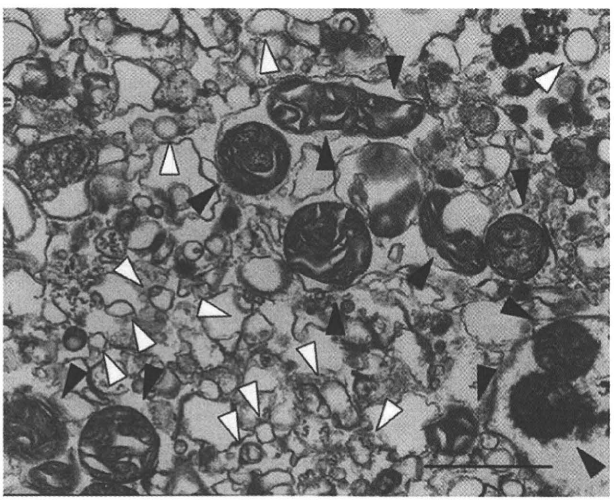

Fig. 4. Electron micrograph of *Paragonimus* mitochondrial preparation with lower densities (Fraction 2, 1.1065 g/ml) fractionated by isopycnic density-gradient (32–52% (w/w) sucrose) centrifugation. Black and white arrowheads indicate mitochondria and microsomal vesicles, respectively. Inserted bar represents 1 μm.

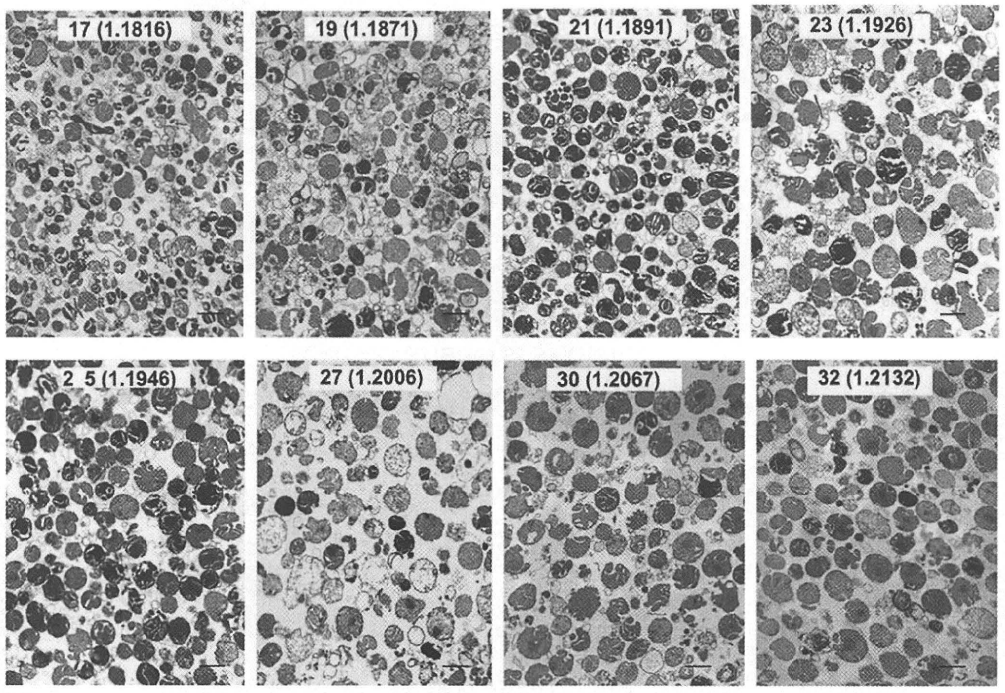

Fig. 5. Electron micrographs of *Paragonimus* mitochondria with higher densities (Fractions 17, 19, 21, 23, 25, 27, 30 and 32) fractionated by isopycnic density-gradient (32–52% (w/w) sucrose) centrifugation. Numbers and numerals in brackets represent fraction numbers and densities, respectively. Inserted bar represents 1 μm.

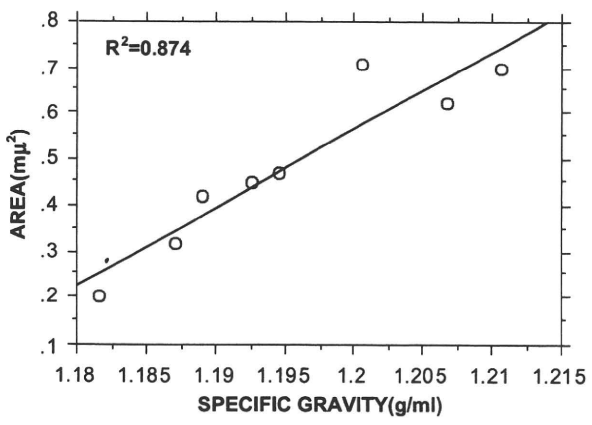

Fig. 6. Relationship between specific gravities and cross-sectional areas of *Paragonimus* mitochondria fractionated by isopycnic density-gradient (32–52% (w/w) sucrose) centrifugation. Medians of mitochondrial cross-sectional areas, as determined by a computer-controlled image analyzer, were plotted against the specific gravities of Fractions 17, 19, 21, 23, 25, 27, 30 and 32. Detailed experimental procedures are described in Section 2.

also detected (Fig. 4). Thus, the specific activity of SQR was lower in Fractions 1–7 than in mitochondria before centrifugation. The specific activity of this mitochondrial marker enzyme in the rest of fractions (Fractions 8–42) ranged from 0.177 (Fraction 8) to 0.595 μmol/min/mg protein (Fraction 22). This variation also suggested heterologous mitochondrial populations that differed in energy metabolism. The average specific activity was calculated to be 0.405 μmol/min/mg, indicating a 2.7-fold purification after centrifugation. Intact rat liver mitochondria have been fractionated by sucrose density gradient ultracentrifugation into two bands, with mean densities of 1.184 and 1.216 g/ml (Pollak and Munn, 1970) and human liver mitochondria exhibited an equilibrium density of 1.20 g/ml (Peters and Seymour, 1978). Thus, the buoyant densities of most fluke mitochondria were similar to those of mammalian aerobic mitochondria.

3.3. Morphological features of fractionated *P. westermani* mitochondria

Since we found that trematode mitochondria were heterologous in situ, we analyzed the morphology of mitochondria fractionated by isopycnic-density-gradient centrifugation. Electron micrographs showed mitochondria that differed in size and staining density; the small mitochondria appeared to be fractionated at lower densities and the large mitochondria at higher densities (Fig. 5). The size (area, μm^2) and staining density (brightness) of individual mitochondrial cross-sections in each fraction were determined one by one using a computer-controlled image analyzer. When we plotted the sizes and brightness of mitochondria versus their densities, we observed a linear relationship (Fig. 6), with small mitochondria present at low sucrose densities and large mitochondria at higher sucrose densities. However, we observed no relationship between the brightness of mitochondria and their density (data not shown). Rather, there were two populations of mitochondria, bright and dark stained, irrespective of their sizes (Figs. 7 and 8). The relative fraction of bright mitochondria appeared to be higher in the high sucrose density fractions, indicating morphological heterogeneity of the fractionated mitochondria.

3.4. Distribution of CCO and FRD activities on separated mitochondria

To further analyze *P. westermani* mitochondria, they were centrifuged on a higher density gradient, i.e., from 35% (w/w) to 55% (w/w) sucrose (Fig. 9). Two linear density gradients were observed, one from Fractions 1 to 6 (1.0865–1.163 g/ml) and the other from Fractions 6 to 37 (1.163–1.253 g/ml). Activities of CCO and FRD, the marker enzymes of the aerobic and anaerobic respiratory chains, were determined in each fraction, and relative ratios of their specific activities were calculated. Mitochondria with high CCO/FRD

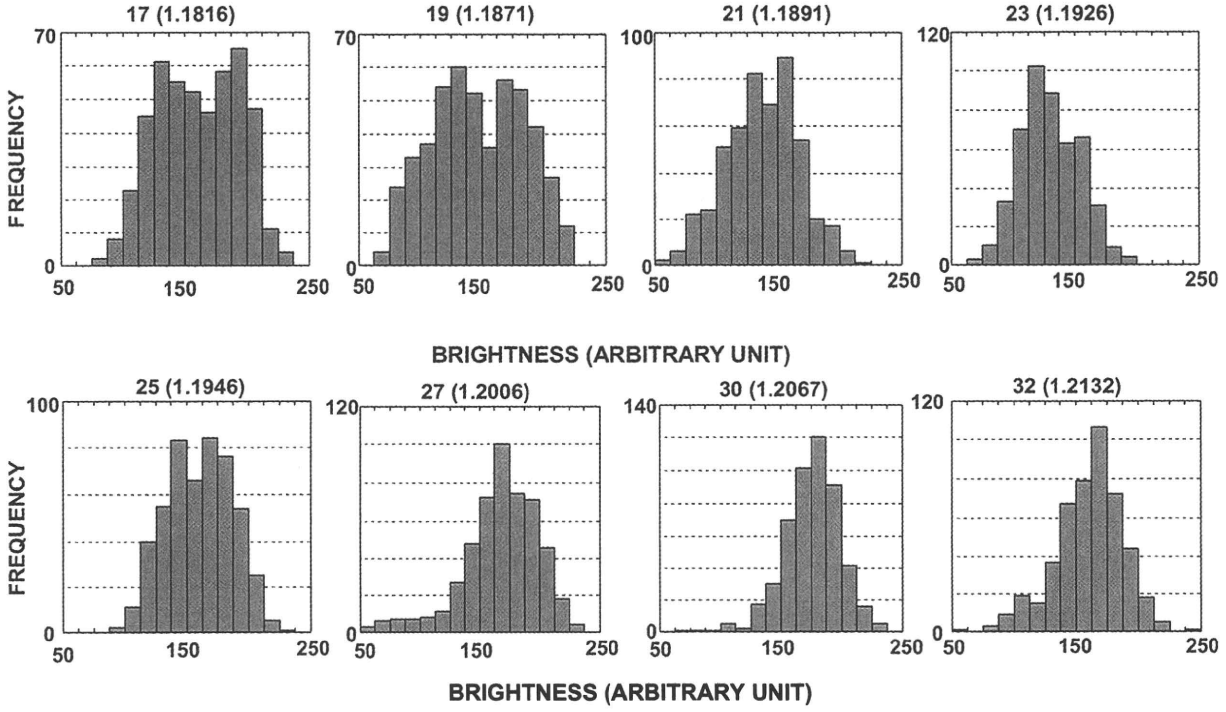

Fig. 7. Histograms of the brightness of *Paragonimus* mitochondria fractionated by isopycnic density-gradient (32–52% (w/w) sucrose) centrifugation. Numbers and numerals in brackets represent fraction numbers and densities, respectively. Brightness of individual mitochondria was determined by a computer-controlled image analyzer. Sample numbers for Fractions 17, 19, 21, 23, 25, 27, 30 and 32 were 477, 491, 502, 479, 502, 502, 502 and 476, respectively.

ratios were mainly recovered at low densities (Fractions 1–7, 1.0865–1.168 g/ml), and those with high FRD/CCO ratios at high densities (Fractions 13–23, 1.192–1.1285 g/ml), indicating that aerobic mitochondria are lighter than anaerobic mitochondria. We also determined the ubiquinone-10 and rhodoquinone-10 contents of fractionated mitochondria to compare the ubiquinone/rhodoquinone ratio in low- and high-density mitochondria. The ubiquinone/rhodoquinone molar ratio was 8.13 and 3.29 in low- and high-density mitochondria, respectively, indicating that the low-density mitochondria are also aerobic in terms of quinone contents.

4. Discussion

Although there have been several studies on the morphological and functional heterogeneity of *Paragonimus* mitochondria (Hamajima et al., 1982; Yamakami et al., 1984; Fujino et al., 1995, 1996), substantial evidence for the occurrence of aerobic and anaerobic mitochondria has been limited. We previously reported that there were three types of mitochondria, which differed in morphology and cytochemistry, in *P. ohirai* tissues (Fujino et al., 1996), but the relationships between morphology and function could not be determined due to limited amounts of material. No direct evidence was presented for Pc2 mitochondria with high FRD activity. By using *P. westermani*, which are larger, for mitochondrial preparation, we were able to further characterise trematode mitochondria. We found that adult *P. westermani* possess three types of mitochondria, small aerobic mitochondria localised in the tegument and tegumental cells and two types of large mitochondria, one localised in Pc1 and highly stained for CCO activity, and the other derived from Pc2 and poorly stained for CCO activity. Fractionation of these trematode mitochondria by isopycnic density-gradient centrifugation based on their buoyant densities, which

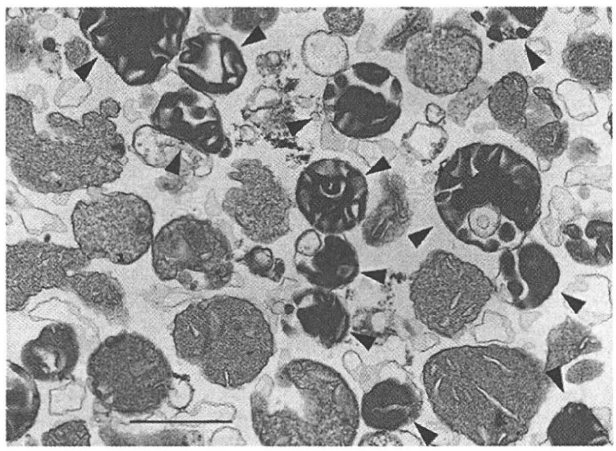

Fig. 8. Electron micrograph of *Paragonimus* mitochondria (Fraction 21) exhibiting different staining densities. Arrowheads show heavily stained mitochondria, with low brightness scores, with the remainder being lightly stained mitochondria, with high brightness scores. Inserted bar represents 1 μm.

are directly proportional to their cross-section areas or sizes, showed that the small mitochondria localised in the tegumental cells were present in the low-density fractions. These mitochondria, of average size $0.180 \pm 0.102\ \mu m^2$, comparable to their in situ average size of $0.130 \pm 0.0819\ \mu m^2$ (Table 1), had high CCO/FRD ratios and well-developed cristae. The parenchymal mitochondria were larger, with in situ sizes of $0.33 \pm 0.193\ \mu m^2$ for Pc1 mitochondria and $0.35 \pm 0.197\ \mu m^2$ for Pc2 mitochondria (Table 1), and were of average size $0.619 \pm 0.314\ \mu m^2$ after gradient fractionation. The larger cross-sectional areas of isolated compared with in situ mitochondria may have been due to unavoidable swelling during isolation.